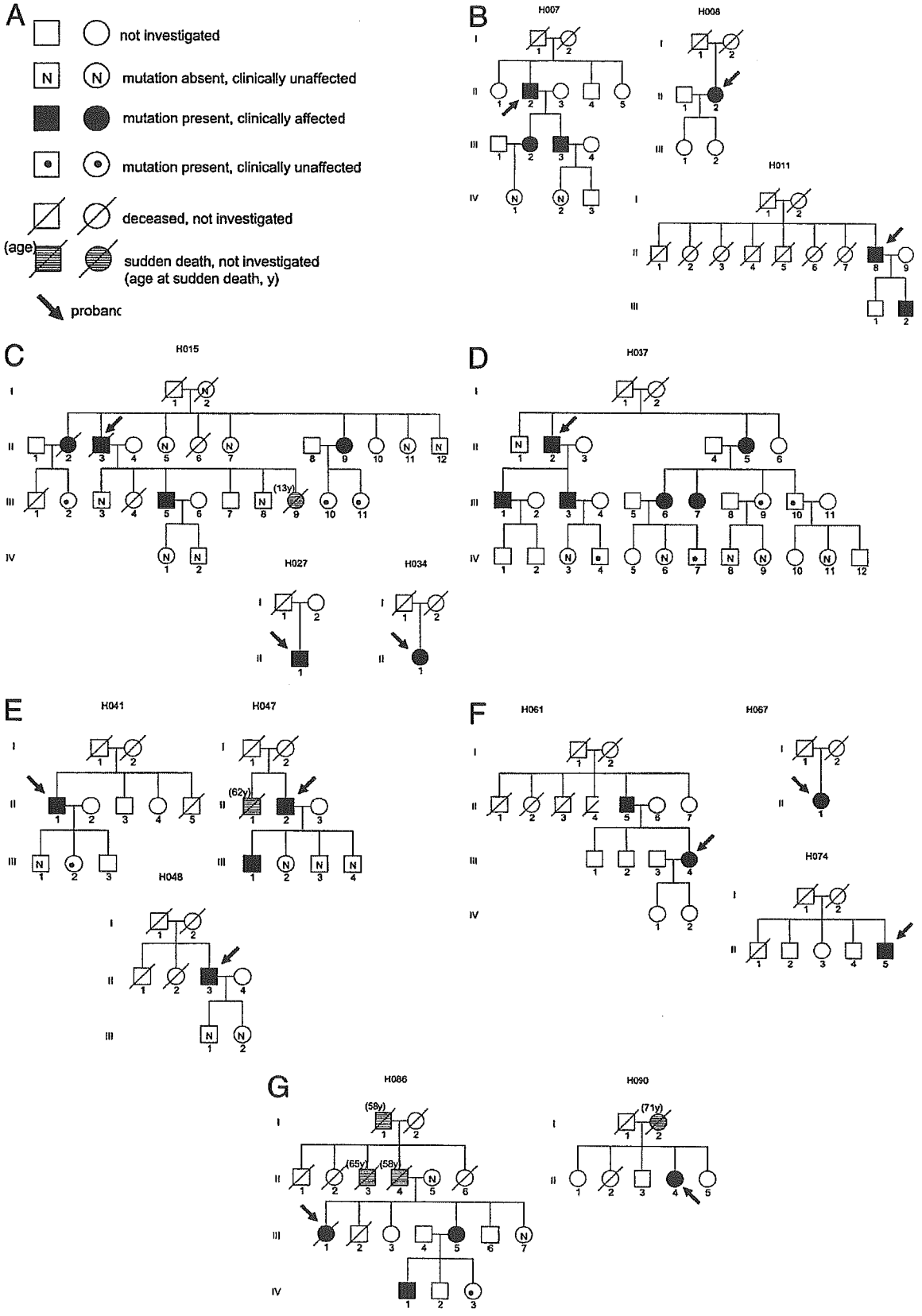


**Figure 1. (A to G)** Pedigree of families H007, H008, H011, H015, H027, H034, H037, H041, H047, H048, H061, H067, H074, H086, and H090. The genotypic status and phenotypic status of subjects are indicated.

JACC Vol. 46, No. 9, 2005
November 1, 2005:1737–43

**Table 1.** Clinical Characteristics of 30 Phenotype-Positive Patients at Presentation

| | |
|---|---|
| Age at presentation, yrs (range) | 48 ± 14 (16–83) |
| Gender: male, n (%) | 17 (57) |
| Age at diagnosis, yrs (range) | 47 ± 15 (14–76) |
| Reason for diagnosis, n (%) | |
| Symptoms | 16 (53) |
| Incidental findings | 4 (13) |
| Family or gene screening | 10 (33) |
| Presence of symptoms, n (%) | 19 (63) |
| Dyspnea, n (%) | 14 (47) |
| Palpitation, n (%) | 11 (37) |
| Syncope, n (%) | 3 (10) |
| Chest pain, n (%) | 7 (23) |
| NYHA functional class | |
| I | 16 (53) |
| II | 10 (33) |
| III and IV | 4 (13) |
| History of AF (chronic or paroxysmal) | 4 (13) |

Data shown as mean value ± SD or number (%).
AF = atrial fibrillation; NYHA = New York Heart Association.

**Clinical manifestation.** Clinical evaluation was performed in the 64 individuals from the 15 proband families studied. The mean follow-up period in the all 39 genotype-positive individuals was 8.0 ± 5.4 years (range, 0.2 to 19.3 years). Thirty patients were phenotype-positive, all with echocardiographic evidence of LVH. Two adults developed hypertrophy (MLVWT ≥13 mm) after the age of 40. Nine of the 39 individuals were not affected phenotypically (average age at last evaluation: 33 ± 11 years; range, 12 to 43 years). The disease penetrance was 100% in subjects ≥50 years and 65% in those <50 years of age.

The clinical characteristics of the 30 phenotype-positive patients at presentation were summarized in Table 1. The age at diagnosis was 47 ± 15 years. Most patients (86%) were evaluated because of symptoms or family screening of HCM. A total of 19 patients (63%) reported cardiac symptoms. Table 2 shows the echocardiographic characteristics of the 30 phenotype-positive patients at presentation and at last follow-up. At presentation, MLVWT was 21 ± 5.3 mm. Six (20%) of those 30 patients had systolic anterior movement of the mitral valve, and three (10%) showed a significant LV outflow tract gradient (pressure gradient at rest ≥30 mm Hg).

Sudden death occurred in six individuals from four families (Fig. 1; families H015, H047, H086, and H090). Three individuals were from one family. Five of them were older than 50 years of age.

**Clinical course.** During a mean follow-up period of 9.2 ± 5.5 years after the first clinical evaluation, paroxysmal or chronic atrial fibrillation (AF) was detected in 10 (33%; incidence, 3.6%/year) of the 30 phenotype-positive patients, eight of whom were 60 years of age or older. Two of those patients experienced severe embolic stroke, which was the cause of their death at the ages of 61 and 68 years, respectively. One patient (H015-II-2) was on oral anticoagulation with warfarin. In the other patient (H086-III-1), AF was detected at the time of the stroke for the first time.

Figure 2 shows longitudinal changes in LVEDD, ejection fraction (EF), and MLVWT in each of the 39 genotype-positive individuals. Figure 2A shows that LVEDD gradually became larger with advancing age. On the other hand, LV systolic function was preserved until middle age. After middle age, reduction of EF occurred in some patients (Fig. 2B). "End-stage" HCM (EF <50%) was observed in seven (18%) of the 39 individuals; six of them were 60 years or older. Five of them showed LVEDD ≥55 mm. Figure 2C shows that MLVWT was thinner in elderly patients than in young patients with HCM and that it was within normal limits in the phenotype-negative individuals.

Table 3 shows the clinical characteristics of seven patients with "end-stage" HCM. More specifically, the average age when they were first identified as in the end-stage phase was 60 years (range, 46 to 70 years). Three patients (H011-II-8, H015-II-3, and H086-III-1) were already in the end-stage phase at presentation. The other four patients progressed to "end-stage" HCM during follow-up. Regarding the cause of LV systolic dysfunction, none of them was considered to have atherosclerotic coronary artery disease because three of them (H007-II-2, H011-II-8 and H086-III-1) had normal coronary angiography, and the remaining four patients had normal thallium-201 myocardial scintigraphy. No one suffered from myocardial infarction. All patients with "end-stage" HCM showed deterioration of New York Heart Association functional class together with a development of paroxysmal or chronic AF at last follow-up. All of them were treated for heart failure and/or arrhythmias: diuretics (n = 6), angiotensin-converting enzyme inhibitors or angiotensin receptor blockers (n = 5), beta-blockers (n = 3), and amiodarone (n = 2). One patient (H007-II-2), who was on amiodarone (maintenance dose 100 to 200 mg/day) for sustained ventricular tachycardia for 10 months, received an implantable cardioverter-

**Table 2.** Echocardiographic Characteristics of 30 Phenotype-Positive Patients

| | At Presentation | At Last Follow-Up |
|---|---|---|
| Age, yrs | 48 ± 14 (16–83) | 56 ± 15 (28–83) |
| MLVWT, mm | 21 ± 5.3 (13–38) | 21 ± 6.0 (13–39) |
| IVST, mm | 19 ± 4.7 (11–28) | 18 ± 4.9 (10–32) |
| PWT, mm | 11 ± 1.7 (7–14) | 11 ± 2.3 (7–19) |
| Left atrial diameter, mm | 40 ± 8.3 (27–60) | 46 ± 9.0 (30–69) |
| LV end-diastolic diameter, mm | 44 ± 7.4 (29–64) | 47 ± 8.1 (37–67) |
| LV end-systolic diameter, mm | 27 ± 7.8 (12–48) | 31 ± 9.2 (21–55) |
| Ejection fraction, % | 66 ± 9.9 (36–85) | 61 ± 13.9 (22–81) |
| Gradient >30 mm Hg, n (%) | 3 (10) | 2 (7) |
| SAM, n (%) | 6 (20) | 6 (20) |
| Pattern of LVH, n | | |
| Asymmetric | 27 | 27 |
| Diffuse | 2 | 1 |
| Apical | 0 | 0 |
| Others | 1 | 2 |

Data shown as mean value ± SD (range) or number (%).
IVST = interventricular septal wall; LV = left ventricular; LVH = left ventricular hypertrophy; MLVWT = maximum left ventricular wall thickness; PWT = left ventricular posterior wall thickness; SAM = systolic anterior movement.

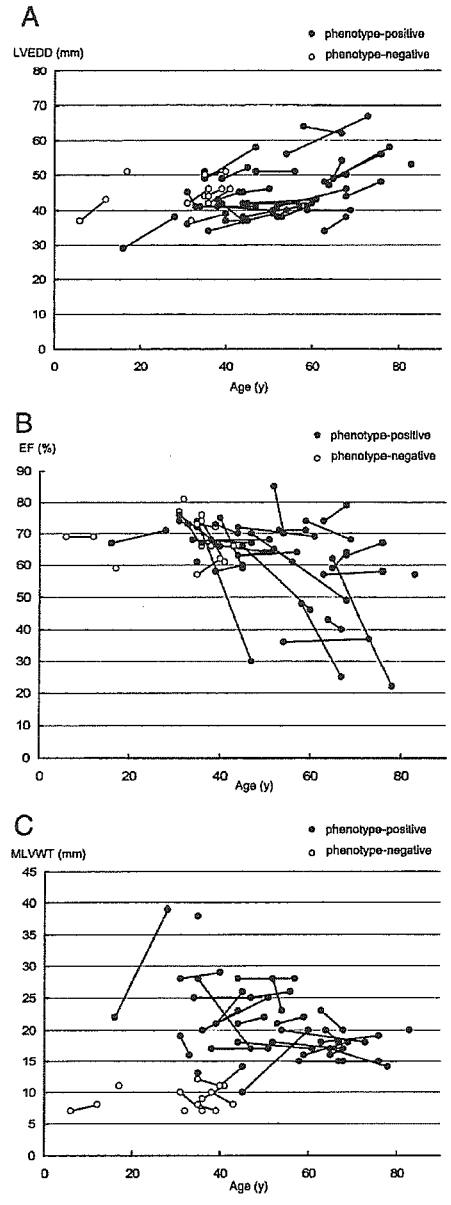


**Figure 2.** Longitudinal echocardiographic changes in 39 genotype-positive individuals during the follow-up period. **(A)** Changes in left ventricular end-diastolic diameter (LVEDD). **(B)** Changes in ejection fraction (EF). **(C)** Changes in maximum left ventricular wall thickness (MLVWT).

**Table 3.** Clinical Characteristics of Seven Patients With "End-Stage" HCM

| Patient | Gender | Age (yrs) at Diagnosis | Age (yrs) at End-Stage | Echocardiography at Initial Evaluation/ at Last Evaluation | | | | NYHA Functional Class, Initial to Last | Rhythm, Initial to Last | Hospitalization for CHF (Age, yrs) | Status (Event Age, yrs) |
|---|---|---|---|---|---|---|---|---|---|---|---|
| | | | | Age (yrs) | LVEDD (mm) | EF (%) | MLVWT (mm) | | | | |
| H007-II-2 | M | 65 | 70 | 65/78 | 49/58 | 62/22 | 17/14 | I to III | SR to AF | + (69) | ICD discharge (76) |
| H007-III-2 | F | 14 | 46 | 35/47 | 49/58 | 74/30 | 28/17 | I to III | SR and PAF | + (46) | Alive |
| H011-II-8 | M | 40 | 58 | 58/68 | 64/62 | 48/25 | 15/17 | II to III | SR to AF | + (63) | Alive, CRT, MVR |
| H015-II-3 | M | 54 | 54 | 54/73 | 56/67 | 36/37 | 20/18 | II to IV | AF to AF | + (54) | CHF death (73) |
| H015-II-2 | F | 45 | 60 | 45/60 | 42/42 | 66/46 | 10/20 | II to III | SR to AF | + (60) | Stroke death (61) |
| H034-II-1 | F | 46 | 68 | 52/68 | 41/46 | 65/49 | 18/17 | I to III | SR to AF | — | Alive |
| H086-III-1 | F | 64 | 64 | 64/67 | 47/55 | 43/40 | 20/18 | II to III | SR to AF | + (64) | Stroke death (68) |

AF = atrial fibrillation; CHF = congestive heart failure; CRT = cardiac resynchronization therapy; EF = ejection fraction; LVEDD = left ventricular end-diastolic diameter; MLVWT = maximum left ventricular wall thickness; MVR = mitral valve replacement; NYHA = New York Heart Association; PAF = paroxysmal AF; SR = sinus rhythm.

defibrillator (ICD) because of amiodarone-induced pulmonary fibrosis. One patient (H011-II-8) underwent mitral valve replacement and cardiac resynchronization therapy for medically-refractory heart failure.

During follow-up (9.2 ± 5.5 years), seven (23%) of the 30 patients (mean age: 62 ± 10 years; range, 46 years to 76 years) were hospitalized for treatment of heart failure, and four patients died or had ICD discharge (one heart failure-death, two stroke-deaths, one ICD discharge; 13%; incidence, 1.4%/year) (Table 3).

## DISCUSSION

Hypertrophic cardiomyopathy is a heterogeneous myocardial disorder and the phenotype is not a static manifestation; LVH can appear at virtually any age and increase or decrease dynamically throughout life (16,20). However, there have been few studies on the phenotype-genotype correlation in terms of longitudinal clinical evaluation. In this study, we examined the clinical courses of patients with a founder mutation (V592fs/8) in the MyBPC gene from 15 unrelated proband families. We observed the longitudinal evolution of phenotype caused by this mutation and concluded that the patients with this mutation were likely to progress to "end-stage" HCM, characterized by LV systolic dysfunction and cavity dilation, with advancing age. To the best of our knowledge this is the first report demonstrating direct longitudinal evolution of phenotype in relation to genotype.

**Disease penetrance and clinical manifestation.** In the present study, the mean age of patients at diagnosis was 47 ± 15 years. During follow-up, two adults showed development of LVH in mid-life, appearing for the first time after 40 years of age. We found that disease penetrance was 100% in subjects ≥50 years and 65% in those <50 years of age. Our data are in accordance with previously reported data for MyBPC mutations (12,14,21–24). Onset of the disease seems to be late in life, although two patients are diagnosed as having the disease at teenagers (H007-III-2 and H047-III-1). These findings indicate that relatives of the patients, even if they are old, should be screened for this mutation. If genetic diagnosis is not available, middle-aged or older relatives of the patients should be evaluated at least every five years for family-screening strategies (2–4,14,25). From a morphologic point of view, the degree of MLVWT varied significantly (13 to 38 mm). None of the subjects showed apical hypertrophy. Sudden death occurred in six individuals from four families in the present study. It is notable that most of sudden deaths occurred in subjects >50 years of age (83%; five of the six individuals) because sudden death occurs most commonly in children and young adults, although the risk extends across a wide age range through mid-life and beyond (3,26,27).

**Clinical course and prognosis.** It was previously suggested that LV remodeling involving some degree of LV cavity enlargement and wall thinning could occur slowly over the course of decades (28–32), although direct longitudinal evidence in relation to gene abnormality was insufficient. In the present study, we were able to demonstrate longitudinal LV remodeling in those with a V592fs/8 mutation and also evolution to "end-stage" HCM in the elderly (Fig. 2). HCM generally has been associated with only mild disability and normal life expectancy if sudden death can be avoided (27,33–35). In this study, the clinical manifestation caused by this mutation was late onset and prognosis was not poor in terms of survival (4 [13%] of the 30 patients died or had ICD discharge; incidence, 1.4%/year). However, a significant subset of the patients is likely to suffer from HCM-related cardiovascular events (repeated heart failure, stroke, and sudden death) later in their lives. The clinical course in patients with this mutation is therefore not benign in the long run, and careful management is needed, particularly in middle-aged and older patients.

**Genotype/phenotype relations.** A V592fs/8 mutation in the MyBPC gene is predicted to result in a truncation of the protein, including loss of C-terminal myosin and titin binding sites (36). Konno et al. (21) recently reported that a missense mutation (Arg820Gln) in the MyBPC gene is responsible for HCM with LV systolic dysfunction and dilation in elderly patients. The function of MyBPC protein has been elucidated by two recent studies using knockout mouse models (37,38). Homozygous-null mice in which full-length MyBPC protein was absent were viable and had significant cardiac hypertrophy with decreased fractional shortening. Furthermore, heterozygous MyBPC-null mice presented a slight-but-significant decrease in MyBPC amount and developed asymmetric septal hypertrophy (38). Thus, we speculate that a collapse of sarcomere stability compensated by residual MyBPC in heterozygous patients may occur with advancing age and may lead to impaired contractile function in the elderly.

Kokado et al. (39) reported that a Lys183 deletion mutation in the troponin I gene in HCM patients was associated with LV systolic impairment and dilation in those older than 40 years of age. Moolman et al. (22) presented that none of the subjects with a single-base insertion in exon 25 of the MyBPC gene showed LV systolic dysfunction and cavity enlargement, although the subjects included several elderly patients. Thus, underlying mutations may relate to the progress to the stage of LV dysfunction and dilation. However, the fact that not all elderly patients with the identical mutation develop "end-stage" disease suggests that other genetic and/or environmental factors are involved and underscores the genetic/phenotypic heterogeneity of HCM. Further investigations are needed to clarify these modifying factors.

**Study limitations.** Whether this particular mutation is more related to the progression to "end-stage" HCM than the other mutations in MyBPC gene or abnormal MyBPC itself is more prone to this phenotype than the other sarcomeric abnormalities is unknown. Further studies on the phenotype-genotype correlation in terms of longitudinal evolution are needed.

**Conclusions.** A founder V592fs/8 mutation in the MyBPC gene was identified in 15 of 94 Japanese families with HCM. Elderly patients in particular may evolve to the "end-stage" HCM, characterized by LV systolic dysfunction, cavity dilation, and irreversible heart failure. Although the manifestation is late in onset, the clinical course in patients with this mutation is not benign in the long run with progressive LV remodeling with advancing age.

**Reprint requests and correspondence:** Dr. Yoshinori L. Doi, Department of Medicine and Geriatrics, Kochi Medical School, Oko-cho, Nankoku-shi, Kochi 783-8505, Japan. E-mail: ydoi@med.kochi-u.ac.jp.

## REFERENCES

1. Spirito P, Seidman CE, McKenna WJ, Maron BJ. The management of hypertrophic cardiomyopathy. N Engl J Med 1997;336:775–85.
2. Maron BJ, McKenna WJ, Danielson GK, et al. American College of Cardiology/European Society of Cardiology clinical expert consensus document on hypertrophic cardiomyopathy. A report of the American College of Cardiology Foundation Task Force on Clinical Expert Consensus Documents and the European Society of Cardiology Committee for Practice Guidelines. J Am Coll Cardiol 2003;42:1687–713.
3. Maron BJ. Hypertrophic cardiomyopathy: a systematic review. JAMA 2002;287:1308–20.
4. Elliott P, McKenna WJ. Hypertrophic cardiomyopathy. Lancet 2004; 363:1881–91.
5. Jarcho JA, McKenna WJ, Pare JA, et al. Mapping a gene for familial hypertrophic cardiomyopathy to chromosome 14q1. N Engl J Med 1989;321:1372–8.
6. Geisterfer-Lowrance AA, Kass S, Tanigawa G, et al. A molecular basis for familial hypertrophic cardiomyopathy: a beta cardiac myosin heavy chain gene missense mutation. Cell 1990;62:999–1006.
7. Kimura A, Harada H, Park JE, et al. Mutations in the cardiac troponin I gene associated with hypertrophic cardiomyopathy. Nat Genet 1997;16:379–82.
8. Towbin JA. Molecular genetics of hypertrophic cardiomyopathy. Curr Cardiol Rep 2000;2:134–40.
9. Bonne G, Carrier L, Richard P, Hainque B, Schwartz K. Familial hypertrophic cardiomyopathy: from mutations to functional defects. Circ Res 1998;83:580–93.
10. Watkins H, Conner D, Thierfelder L, et al. Mutations in the cardiac myosin binding protein-C gene on chromosome 11 cause familial hypertrophic cardiomyopathy. Nat Genet 1995;11:434–7.
11. Bonne G, Carrier L, Bercovici J, et al. Cardiac myosin binding protein-C gene splice acceptor site mutation is associated with familial hypertrophic cardiomyopathy. Nat Genet 1995;11:438–40.
12. Niimura H, Bachinski LL, Sangwatanaroj S, et al. Mutation in the gene for cardiac myosin-binding protein C and late-onset familial hypertrophic cardiomyopathy. N Engl J Med 1998;338:1248–57.
13. Arad M, Seidman JG, Seidman CE. Phenotypic diversity in hypertrophic cardiomyopathy. Hum Mol Genet 2002;11:2499–506.
14. Maron BJ, Niimura H, Casey SA, et al. Development of left ventricular hypertrophy in adults with hypertrophic cardiomyopathy caused by cardiac myosin-binding protein C gene mutations. J Am Coll Cardiol 2001;38:315–21.
15. Van Driest SL, Vasile VC, Ommen SR, et al. Myosin binding protein C mutations and compound heterozygosity in hypertrophic cardiomyopathy. J Am Coll Cardiol 2004;44:1903–10.
16. Maron BJ, Spirito P. Implications of left ventricular remodeling in hypertrophic cardiomyopathy. Am J Cardiol 1998;81:1339–44.
17. Doi YL, Kitaoka H, Hitomi N, Satoh M, Kimura A. Clinical expression in patients with hypertrophic cardiomyopathy caused by cardiac myosin-binding protein C gene mutation. Circulation 1999; 100:448–9.
18. Shapiro LM, McKenna WJ. Distribution of left ventricular hypertrophy in hypertrophic cardiomyopathy: a two-dimensional echocardiographic study. J Am Coll Cardiol 1983;2:437–44.
19. Maron BJ, Gottdiener JS, Epstein SE. Patterns and significance of distribution of left ventricular hypertrophy in hypertrophic cardiomyopathy. A wide angle, two dimensional echocardiographic study of 125 patients. Am J Cardiol 1981;48:418–28.
20. Ogimoto A, Hamada M, Nakura J, et al. 17-year follow-up study of a patient with obstructive hypertrophic cardiomyopathy with a deletion mutation in the cardiac myosin binding protein C gene. Circ J 2004;68:174–7.
21. Konno T, Shimizu M, Ino H, et al. A novel missense mutation in the myosin binding protein-C gene is responsible for hypertrophic cardiomyopathy with left ventricular dysfunction and dilation in elderly patients. J Am Coll Cardiol 2003;41:781–6.
22. Moolman JA, Reith S, Uhl K, et al. A newly created splice donor site in exon 25 of the MyBP-C gene is responsible for inherited hypertrophic cardiomyopathy with incomplete disease penetrance. Circulation 2000;101:1396–402.
23. Erdmann J, Raible J, Maki-Abadi J, et al. Spectrum of clinical phenotypes and gene variants in cardiac myosin-binding protein C mutation carriers with hypertrophic cardiomyopathy. J Am Coll Cardiol 2001;38:322–30.
24. Charron P, Dubourg O, Desnos M, et al. Clinical features and prognostic implications of familial hypertrophic cardiomyopathy related to the cardiac myosin-binding protein C gene. Circulation 1998;97:2230–6.
25. Maron BJ, Seidman JG, Seidman CE. Proposal for contemporary screening strategies in families with hypertrophic cardiomyopathy. J Am Coll Cardiol 2004;44:2125–32.
26. Elliott PM, Poloniecki J, Dickie S, et al. Sudden death in hypertrophic cardiomyopathy: identification of high risk patients. J Am Coll Cardiol 2000;36:2212–8.
27. Maron BJ, Olivotto I, Spirito P, et al. Epidemiology of hypertrophic cardiomyopathy-related death: revisited in a large non-referral-based patient population. Circulation 2000;102:858–64.
28. Spirito P, Maron BJ. Relation between extent of left ventricular hypertrophy and age in hypertrophic cardiomyopathy. J Am Coll Cardiol 1989;13:820–3.
29. Lewis JF, Maron BJ. Elderly patients with hypertrophic cardiomyopathy: a subset with distinctive left ventricular morphology and progressive clinical course late in life. J Am Coll Cardiol 1989;13:36–45.
30. Lever HM, Karam RF, Currie PJ, Healy BP. Hypertrophic cardiomyopathy in the elderly. Distinctions from the young based on cardiac shape. Circulation 1989;79:580–9.
31. Fay WP, Taliercio CP, Ilstrup DM, Tajik AJ, Gersh BJ. Natural history of hypertrophic cardiomyopathy in the elderly. J Am Coll Cardiol 1990;16:821–6.
32. Thaman R, Gimeno JR, Reith S, et al. Progressive left ventricular remodeling in patients with hypertrophic cardiomyopathy and severe left ventricular hypertrophy. J Am Coll Cardiol 2004;44:398–405.
33. Spirito P, Chiarella F, Carratino L, Berisso MZ, Bellotti P, Vecchio C. Clinical course and prognosis of hypertrophic cardiomyopathy in an outpatient population. N Engl J Med 1989;320:749–55.
34. Maron BJ, Casey SA, Poliac LC, Gohman TE, Almquist AK, Aeppli DM. Clinical course of hypertrophic cardiomyopathy in a regional United States cohort. JAMA 1999;281:650–5.
35. Cecchi F, Olivotto I, Montereggi A, Santoro G, Dolara A, Maron BJ. Hypertrophic cardiomyopathy in Tuscany: clinical course and outcome in an unselected regional population. J Am Coll Cardiol 1995;26:1529–36.
36. Flashman E, Redwood C, Moolman-Smook J, Watkins H. Cardiac myosin binding protein C: its role in physiology and disease. Circ Res 2004;94:1279–89.
37. Harris SP, Bartley CR, Hacker TA, et al. Hypertrophic cardiomyopathy in cardiac myosin binding protein-C knockout mice. Circ Res 2002;90:594–601.
38. Carrier L, Knoll R, Vignier N, et al. Asymmetric septal hypertrophy in heterozygous cMyBP-C null mice. Cardiovasc Res 2004;63:293–304.
39. Kokado H, Shimizu M, Yoshio H, et al. Clinical features of hypertrophic cardiomyopathy caused by a Lys183 deletion mutation in the cardiac troponin I gene. Circulation 2000;102:663–9.

Available online at www.sciencedirect.com
SCIENCE DIRECT
ELSEVIER
Biomedicine & Pharmacotherapy 59 (2005) S49–S53
BIOMEDICINE & PHARMACOTHERAPY
http://france.elsevier.com/direct/BIOPHA/

# Common carotid intima–media thickness is predictive of all-cause and cardiovascular mortality in elderly community-dwelling people: Longitudinal Investigation for the Longevity and Aging in Hokkaido County (LILAC) study

S. Murakami [a, b, c], K. Otsuka [a, b, *], N. Hotta [a, b], G. Yamanaka [a], Y. Kubo [a], O. Matsuoka [a], T. Yamanaka [a, b], M. Shinagawa [a], S. Nunoda [a], Y. Nishimura [a], K. Shibata [a, b], E. Takasugi [a, b], M. Nishinaga [d], M. Ishine [e], T. Wada [e], K. Okumiya [f], K. Matsubayashi [g], S. Yano [h], K. Ichihara [i], G. Cornélissen [j], F. Halberg [j]

[a] *Department of Medicine, Medical Center East, Tokyo Women's Medical University, Nishiogu 2-1-10, Arakawa, Tokyo 116-8567, Japan*
[b] *Division of Neurocardiology and Chronoecology, Medical Center East, Tokyo Women's Medical University, Nishiogu 2-1-10, Arakawa, Tokyo 116-8567, Japan*
[c] *Department of Internal Medicine, Osaka Medical University, Osaka, Japan*
[d] *Department of Gerontology, School of Medicine, Kochi University, Kochi, Japan*
[e] *Department of Field Medicine, Kyoto University Graduate School of Medicine, Kyoto, Japan*
[f] *Research Institute for Humanity and Nature, Kyoto, Japan*
[g] *Center for South-East Asian Studies, Kyoto University, Kyoto, Japan*
[h] *Sorachi Health and Welfare Office, Sorachi-Godochosha, Iwamizawa, Hokkaido, Japan*
[i] *Division of Clinical Laboratory Sciences, Faculty of Health Sciences, School of Medicine, Yamaguchi University, Ube, Japan*
[j] *Halberg Chronobiology Center, University of Minnesota, Minneapolis, MN, USA*

**Abstract**

Several cohort studies have examined the association of carotid intima–media thickness (IMT) with the risk of stroke or myocardial infarction in apparently healthy persons. We investigated the predictive value of IMT of cardiovascular mortality in elderly community-dwelling people, beyond the prediction provided by age and MMSE, assessed by means of a multivariate Cox model. Carotid IMT and plaque were evaluated bilaterally with ultrasonography in 298 people older than 75 years (120 men and 178 women, average age: 79.6 years). The LILAC study started on July 25, 2000. Consultations were repeated every year. The follow-up ended on November 30, 2004. During the mean follow-up span of 1152 days, 30 subjects (21 men and nine women) died. Nine deaths were attributable to cardiovascular causes (myocardial infarction: two men and three women; stroke: two men and two women). The age- and MMSE-adjusted relative risk (RR) and 95% confidence interval (95% CI) of developing all-cause mortality was assessed. A 0.3 mm increase in left IMT was associated with a RR of predicted 1.647 (1.075–2.524), and a similar increase in right IMT with a RR of 3.327 (1.429–7.746). For cardiovascular mortality, the corresponding RR values were 2.351 (1.029–5.372) and 2.890 (1.059–7.891), respectively. Carotid IMT assessed by ultrasonography is positively associated with an increased risk of all-cause and cardiovascular death in elderly community-dwelling people.


*Keywords:* Carotid intima–media thickness; All-cause mortality; Cardiovascular mortality; Cognitive function; Elderly community-dwelling people

* Corresponding author.
*E-mail address:* otsukagm@dnh.twmu.ac.jp (K. Otsuka).

## 1. Introduction

Several prospective population-based studies documented that carotid intima–media thickness (IMT) was positively associated with stroke and myocardial infarction in highly selected patients. Carotid IMT has also been shown to predict fatal coronary death and fatal stroke in elderly people [1–5]. It is now considered to constitute a surrogate marker of cardiovascular morbidity and mortality risk not only in patients, but also quite generally in young, middle-aged and elderly populations.

In 2000, we began a community-based study to Longitudinally Investigate the Longevity and Aging in Hokkaido County (LILAC), and to evaluate the population's neurocardiological function. Our goal is the prevention of cardiovascular events, including stroke and myocardial ischemic events, to prevent the decline in cognitive function of the elderly in a community dwelling. In this investigation, we estimated the ability of carotid IMT to predict all-cause and cardiovascular mortality in an elderly population. We already found that the cognitive function, estimated by MMSE and HDS-R, and age statistically significantly predicted cardiovascular death in this population. Herein, we examine the predictive value of all-cause and cardiovascular mortality offered by the carotid IMT, beyond the prediction provided by age and MMSE, as assessed by means of a multivariate Cox model.

## 2. Methods

### 2.1. Subjects and LILAC study design

We examined 298 subjects (120 men and 178 women) older than 75 years (average age: 79.6 years). BP was measured at the beginning of the study in a sitting position, and the brachial-ankle PWV (baPWV) was measured between the right arm and ankle in a supine position, using an ABI/Form instrument (Nippon Colin Co., Ltd., Komaki, Japan). The baPWV was measured using a volume-plethysmographic method. baPWV was measured in duplicate after at least a 5-min rest. Only baPWV measurements from participants with normal ankle/brachial pressure index (ABI) values (>0.90) were considered. The maximal value among the four readings was used for analysis. An echocardiogram and a conventional ECG record were also obtained as usual.

### 2.2. Carotid artery assessment

To measure the carotid intima–media thickness, ultrasonography of the common carotid artery, carotid bifurcation, and internal carotid artery of the left and right carotid arteries was performed with a 7.5-MHz linear-array transducer (SonoSite 180PLUS, Olympus, Tokyo). On a longitudinal, two-dimensional ultrasound image of the carotid artery, the anterior (near) and posterior (far) walls of the carotid artery are displayed as two bright white lines separated by a hypoechogenic space. The distance between the leading edge of the first bright line of the far-wall (lumen–intima interface) and the leading edge of the second bright line (media–adventitia interface) indicates the intima–media thickness. For the near-wall, the distance between the trailing edge of the first bright line and the trailing edge of the second bright line at the near-wall provides the best estimate of the near-wall intima–media thickness. When an optimal longitudinal image was obtained, it was frozen and the frozen images were digitized. The beginning of the dilatation of the distal common carotid artery served as a reference point for the start of measurement. The average of the intima–media thickness of each of the three frozen images was calculated. For each individual, the common carotid intima–media thickness was determined as the average of near- and far-wall measurements of both the left and right arteries. Usual lumen parameters including the common carotid artery (CCA), systolic peak velocity (VPS) and end-diastolic velocity (VED), measured by Doppler ultrasonogram, and the resistive index (RI) were also measured.

### 2.3. Heart rate variability

The first 1-h record of an ambulatory ECG obtained during routine medical examination conducted each year in July was processed for HRV, using a Fukuda-Denshi Holter analysis system (SCM-280-3). Time-domain (SDNN) and frequency-domain (spectral power in the "very low frequency" – VLF: 0.003–0.04 Hz, "low frequency" – LF: 0.04–0.15 Hz, and "high frequency" – HF: 0.15–0.40 Hz regions, and the LF/HF ratio) measures were determined. SDNN was calculated over the whole 1-h record, whereas the frequency-domain endpoints were computed as averages from estimates obtained over consecutive 5-min intervals. Spectral indices were obtained by the maximum entropy method (MEM) with the MemCalc/CHIRAM program (Suwa Trust Co., Ltd., Tokyo, Japan).

The Japanese version of the Mini-Mental State Examination (MMSE) and the Hasegawa Dementia Scale Revised (HDSR) were used to assess the overall cognitive function, including verbal orientation, memory, and constructional ability (Kohs block test). The Up & Go test measured, in seconds, the time it took the subject to stand up from a chair, walk a distance of 3 m, turn, walk back to the chair, and sit down again. This test is a simple measure of physical mobility and demonstrates the subject's balance, gait speed, and functional ability (Up & Go). A lower time score indicates better physical mobility. Functional Reach (FR), used to evaluate balance, represents the maximal distance a subject can reach forward beyond arm's length while maintaining a fixed base of support in the standing position. A higher score indicates better balance. Manual dexterity was assessed using a panel with combinations of 10 hooks, 10 big buttons, and five small buttons. There were three discrete measurements of time recorded for each participant (10 "hook-on"s, 10 big "button-on-and-off"s, and five small "button-on-and-off"s). The total manual dexterity time in seconds, defined as the button score (Button-S), was calcu-

lated by adding the average times for one hook-on and one big or small button-on-and-off. A lower button score indicates better manual dexterity.

### 2.4. All-cause and cardiovascular mortality

The follow-up span herein ended on November 30, 2004. The follow-up time was defined as the time elapsed between the date of the first (reference) examination and the date of death.

### 2.5. Statistical analysis

All data were analyzed with the Statistical Software for Windows (StatFlex Ver.5.0, Artec, Osaka, http://www.statflex.net). We used Cox regression analysis to calculate the unadjusted or adjusted relative risk (RR) and corresponding 95% confidence interval (CI) for all-cause and cardiovascular mortality. To identify independent predictors of mortality, we used multivariate Cox regression analyses with stepwise selection. Variables included in the multivariate models were age, gender, BMI and HR variability indices. Significance was considered at a value of $P < 0.05$.

## 3. Results

During the mean follow-up time of 1152 days, 30 subjects (21 men and nine women) died. Nine deaths were attributable to cardiovascular causes (myocardial infarction: two men and three women; stroke: two men and two women).

### 3.1. All-cause mortality

Among the variables considered herein, Cox proportional hazard models adjusted for age and MMSE found a statistically significant association with all-cause mortality only for gender, baPWV and carotid IMT, Table 1 (left). Being a man had a relative risk of 3.570 (95% CI: 1.619–7.874). A 200 or 500 cm/s increase in baPWV was associated with a relative risk of 1.122 (95% CI: 1.001–1.258) or 1.333 (95% CI: 1.002–1.774), respectively. A 0.2 or 0.3 mm increase in left carotid IMT was associated with a relative risk of 1.395 (95% CI: 1.049–1.854) or 1.647 (95% CI: 1.075–2.524), respectively. For the right carotid IMT, the relative risk was 2.228 (95% CI: 1.268–3.915) or 3.327 (95% CI: 1.429–7.746), respectively.

### 3.2. Cardiovascular mortality

Age- and MMSE-adjusted predictors of cardiovascular mortality were found to be baPWV and the carotid IMT, Table 1 (right). A 200 or 500 cm/s increase in baPWV was associated with a relative risk of 1.321 (95% CI: 1.120–1.558) or 2.005 (95% CI: 1.327–3.031), respectively. A 0.2 or 0.3 mm increase in left carotid IMT was associated with a relative risk of 1.768 (95% CI: 1.019–3.067) or 2.351 (95% CI: 1.029–5.372), respectively. For the right carotid IMT, the relative risk was 2.029 (95% CI: 1.039–3.963) or 2.890 (95% CI: 1.059–7.891), respectively.

## 4. Discussion

The findings herein indicate that in elderly community-dwelling people, independently of cognitive function, an increased common carotid IMT is associated with an elevated risk of both all-cause and cardiovascular mortality. Among the many variables considered in this study, including lumen parameters of the carotid artery, various kinds of parameters of echocardiography, heart rate variability, QT interval, behavioral activities (Up and Go, functional reach and button test), time perception and depressive mood, it is noteworthy that only carotid IMT and baPWV predicted the occurrence of all-cause mortality and cardiovascular death. It is important to realize that arterial blood flow in the common carotid artery, estimated by systolic peak velocity, end-diastolic velocity and the resistive index is virtually normal in these subjects. Kuller et al. [6] showed a considerably increased risk of cardiovascular morbidity and mortality for subjects with subclinical disease compared with subjects with no signs of subclinical disease. These results are in accordance with our finding that among subjects free from symptomatic cerebrovascular and cardiovascular disease, an increased IMT is associated with an increased risk of cardiovascular mortality.

To our knowledge, this is the first prospective study for a community-dwelling population to demonstrate statistically significant associations with cardiovascular mortality of carotid atherosclerosis, in a multivariate Cox model adjusted for cognitive function. It is also noteworthy that carotid IMT predicted not only cardiovascular mortality but also all-cause mortality. Since an impaired cognitive function was associated with all-cause mortality in several populations, our observation after adjustment for age and MMSE may have applications in clinical practice.

Several cross-sectional studies [7] have shown that increased common carotid IMT may be useful as a marker of atherosclerosis elsewhere in the arterial system, in keeping with our finding that not only carotid IMT but also baPWV conferred an increased risk of cerebro- and cardiovascular mortality. It should be noted that the relative risk of an increased IMT was higher than that of an increased baPWV, suggesting that IMT may be a better predictor than baPWV. baPWV is a novel noninvasive technique assessing pulse wave transmission between the brachial and tibial arteries [8]. It is considered to be an indicator of arterial stiffness and a marker of vascular damage [9].

Our data suggest that measurement of IMT in subclinical subjects may be useful to obtain an estimate of mortality risk that is more precise than that based on the measurement of conventional risk factors alone, and may thus have additional predictive value. In addition, using IMT as a primary outcome measure in intervention trials on the efficacy of blood pressure or lipid lowering regimens, especially from the viewpoint of chronodiagnosis and chronotherapy, may lead to major applications in clinical practice to reduce the progression of atherosclerosis.

Table 1
Age- and MMSE-adjusted relative risk of all-cause and cardiovascular mortality in elderly population

| Variables | All-cause mortality | | | | Cardiovascular mortality | | | |
|---|---|---|---|---|---|---|---|---|
| | n | RR | 95% CI | *P*-value | n | RR | 95% CI | *P*-value |
| Gender | 291 | 3.570 | 1.619–7.874 | 0.0016 | 271 | | | N.S. |
| BMI | 279 | | | N.S. | 260 | | | N.S. |
| SBP | 279 | | | N.S. | 259 | | | N.S. |
| DBP | 278 | | | 0.0733 | 259 | | | N.S. |
| PP | 278 | | | N.S. | 259 | | | N.S. |
| Postural BP change | 276 | | | 0.0818 | 256 | | | 0.0818 |
| Pulse rate | 279 | | | N.S. | 259 | | | N.S. |
| Up and Go | 288 | | | N.S. | 269 | | | N.S. |
| FR | 287 | | | N.S. | 268 | | | N.S. |
| Button | 289 | | | N.S. | 269 | | | N.S. |
| HDSR | 291 | | | N.S. | 271 | | | 0.0762 |
| Kohs | 272 | | | N.S. | 253 | | | N.S. |
| GDS | 273 | | | N.S. | 254 | | | N.S. |
| Time estimation (60A) | 258 | | | N.S. | 244 | | | N.S. |
| Time estimation (60B) | 252 | | | N.S. | 240 | | | N.S. |
| HR | 243 | | | N.S. | 229 | | | N.S. |
| VLF | 191 | | | N.S. | 182 | | | N.S. |
| LF | 189 | | | N.S. | 180 | | | N.S. |
| HF | 192 | | | N.S. | 183 | | | N.S. |
| LF/HF | 192 | | | 0.0936 | 183 | | | 0.0936 |
| SDNN | 191 | | | N.S. | 182 | | | N.S. |
| Lown | 273 | | | N.S. | 253 | | | N.S. |
| PWV (200) | 242 | 1.122 | 1.001–1.258 | 0.0487 | 223 | 1.321 | 1.120–1.558 | 0.0010 |
| PWV (500) | 242 | 1.333 | 1.002–1.774 | 0.0487 | 223 | 2.005 | 1.327–3.031 | 0.0010 |
| ABI | 260 | | | N.S. | 241 | | | N.S. |
| IMT Lt (0.1) | 130 | 1.181 | 1.024–1.362 | 0.0220 | 128 | 1.330 | 1.010–1.751 | 0.0426 |
| IMT Lt (0.2) | 130 | 1.395 | 1.049–1.854 | 0.0220 | 128 | 1.768 | 1.019–3.067 | 0.0426 |
| IMT Lt (0.3) | 130 | 1.647 | 1.075–2.524 | 0.0220 | 128 | 2.351 | 1.029–5.372 | 0.0426 |
| IMT Rt (0.1) | 129 | 1.493 | 1.126–1.979 | 0.0053 | 126 | 1.424 | 1.019–1.991 | 0.0383 |
| IMT Rt (0.2) | 129 | 2.228 | 1.268–3.915 | 0.0053 | 126 | 2.029 | 1.039–3.963 | 0.0383 |
| IMT Rt (0.3) | 129 | 3.327 | 1.429–7.746 | 0.0053 | 126 | 2.890 | 1.059–7.891 | 0.0383 |
| Lt CCA | 131 | | | 0.0682 | 128 | | | N.S. |
| Rt CCA | 127 | | | 0.0699 | 124 | | | N.S. |
| Lt VPS | 130 | | | N.S. | 127 | | | N.S. |
| Rt VPS | 129 | | | N.S. | 126 | | | N.S. |
| Lt VED | 130 | | | N.S. | 127 | | | N.S. |
| Rt VED | 128 | | | N.S. | 125 | | | N.S. |
| Lt RI | 123 | | | N.S. | 120 | | | N.S. |
| Rt RI | 114 | | | 0.1069 | 111 | | | N.S. |
| LVMI | 135 | | | N.S. | 126 | | | N.S. |
| Calcification of M-valve | 151 | | | N.S. | 141 | | | N.S. |
| Calcification of A-valve | 150 | | | N.S. | 140 | | | N.S. |
| LVDd | 135 | | | N.S. | 126 | | | N.S. |
| %FS | 135 | | | N.S. | 126 | | | N.S. |
| EF | 135 | | | N.S. | 126 | | | N.S. |
| E | 146 | | | N.S. | 137 | | | N.S. |
| A | 146 | | | N.S. | 137 | | | N.S. |
| E/A | 146 | | | 0.0624 | 137 | | | N.S. |
| DT | 143 | | | N.S. | 134 | | | N.S. |
| QTd | 134 | | | N.S. | 125 | | | N.S. |
| QT | 177 | | | N.S. | 167 | | | 0.0505 |
| QTc | 175 | | | N.S. | 165 | | | N.S. |

Gender: male versus female; Lt = left; Rt = right.

We conclude that carotid IMT assessed by ultrasonography is positively associated with an increased risk of all-cause mortality and cardiovascular death in particular. This study provides supportive evidence for the use of IMT measurements as an intermediate endpoint in intervention trials.

## Acknowledgements

This study was supported by (1) Japan Arteriosclerosis Prevention Fund and (2) Fukuda Foundation for Medical (Grant in 2004 for the study on association between arterial stiffness and cognitive impairment in community-dwelling subjects over 70 years old).

## References

[1] Chambless LE, Heiss G, Folsom AR. Association of coronary heart disease incidence with carotid artery wall thickness and major risk factors: the Atherosclerosis Risk in Communities (ARIC) study, 1987–1993. Am J Epidemiol 1997;146:483–94.

[2] Bots ML, Hoes AW, Koudstaal PJ, Hofman A, Grobbee DE. Common carotid intima–media thickness and risk of stroke and myocardial infarction. The Rotterdam study. Circulation 1997;96:1432–7.

[3] Hodis HN, Mack WJ, LaBree L, Seizer RH, Liu C-r, Liu C-h, et al. The role of carotid arterial intima–media thickness in predicting clinical coronary events. Ann Intern Med 1998;128:262–9.

[4] Chambless LE, Folsom AR, Clegg LX, Sharrett AR, Shahar E, Nieto FJ, et al. Carotid wall thickness is predictive of incident clinical stroke: the Atherosclerosis Risk in Communities (ARIC) study. Am J Epidemiol 2000;15:478–87.

[5] Kitamura A, Iso H, Imano H, Ohira T, Okada T, Sato S, et al. Carotid intima–media thickness and plaque characteristics as a risk factor for stroke in Japanese elderly men. Stroke 2004;35:2788–94.

[6] Kuller LH, Shemanski L, Psaty BM, Borhani NO, Gardin J, Haan MN, et al. Subclinical disease as an independent risk factor for cardiovascular disease. Circulation 1995;92:720–6.

[7] Bots ML, Witteman JCM, Grobbee DE. Carotid intima–media wall thickness in elderly women with and without atherosclerosis of the abdominal aorta. Atherosclerosis 1993;102:99–105.

[8] Yamashina A, Tomiyama H, Takeda K, Tsuda H, Arai T, Hirose K, et al. Validity, reproducibility, and clinical significance of noninvasive brachial-ankle pulse wave velocity measurement. Hypertens Res 2002;25:359–64.

[9] Asmar R. Arterial stiffness and pulse wave velocity. Amsterdam: Elsevier, 1999, pp. 9–15.

J Rehabil Med 2004; 36: 42–45

Taylor&Francis
healthsciences

# VERTICAL GROUND REACTION FORCE SHAPE IS ASSOCIATED WITH GAIT PARAMETERS, TIMED UP AND GO, AND FUNCTIONAL REACH IN ELDERLY FEMALES

Toshiaki Takahashi,[1] Kenji Ishida,[1] Daisuke Hirose,[1] Yasunori Nagano,[1] Kiyoto Okumiya,[2] Masanori Nishinaga,[2] Yoshinori Doi[2] and Hiroshi Yamamoto[1]

*From the [1]Department of Orthopaedic Surgery, Kochi Medical School, Kochi, [2]Department of Medicine and Geriatrics, Kochi Medical School, Kochi, Japan*

***Objective:*** **The aim of this study was to evaluate the relationship between knee pain and various indicators of the combined performance of the lower extremity (including gait parameters, functional performance such as timed up and go, and functional reach test) and to determine whether the classification of vertical ground reaction forces correlates with gait parameters and functional performance.**

***Subjects and Methods:*** **Simultaneous analysis of gait, time-distance parameters and vertical ground reaction force. Timed up and go, and functional reach test were examined in 130 elderly women. The vertical component of the ground reaction force was grouped into 2 categories: M-shaped and non-M-shaped.**

***Results:*** **No significant association was found between knee pain and timed up and go, functional reach test, or gait parameters in elderly female participants. There were significant differences between subjects with M- and non-M-shaped vertical ground reaction forces with regard to timed up and go, functional reach test and Japan Orthopaedic Association score. There were also significant differences between the 2 groups (M shaped and non-M-shaped) in gait parameters.**

***Conclusion:*** **Evaluation of the vertical ground reaction force to determine its shape may be a useful and simple tool in the analysis of gait and functional performance.**

*Key words:* knee pain, gait analysis, elderly females, ground reaction force, osteoarthritis.

J Rehabil Med 2004; 36: 42–45

*Correspondence address: Toshiaki Takahashi, Department of Orthopaedic Surgery, Kochi Medical School, Oko-cho, Nankoku, Kochi, 783-8505, Japan. E-mail: takahast@kochi-ms.ac.jp*

Submitted January 22, 2003; Accepted August 25, 2003

## INTRODUCTION

Osteoarthritis of the knee is one of the most common diseases in elderly females. There are several ways of testing locomotor function of the lower extremity, including measures of muscle strength, gait analysis and some types of knee evaluation scales (1–3). However, there is limited evidence that these parameters are highly correlated with the functional state of the knee. Gait analysis is becoming recognized as an important clinical tool in orthopaedics, in pre-surgery planning, post-surgery monitoring and in a posterior evaluation of various corrective interventions (4, 5). However, it is sometimes difficult for clinicians to analyse the large amounts of data gathered in the assessment of gait time and distance parameters (5).

Objective quantitative assessment of mobility and balance is important for older people because problems with gait and balance can result in a restriction of activity. The Timed Up and Go (TUG) test correlates with gait speed, balance and movement of the lower extremities (6). The Functional Reach (FR) test is a simple measurement of standing balance that can predict falls in elderly people (7, 8).

There have been several reports concerning gait analysis in osteoarthritis of the knee (1, 9). The vertical ground reaction force (VGRF) has been shown to be a reliable and repeatable feature of gait (10–11). There have been numerous studies regarding ground reaction forces during walking (12–14). Gait speed significantly affects VGRF (12, 13, 16). The VGRF varies continually from the instant of initial contact until the foot leaves the supporting surface (17). Body mass, proportions, walking style and balance all affect VGRF (17).

There have been only a few reports regarding the relationship between VGRF and various gait parameters in elderly females with osteoarthritic knees. Analyses that include a classification of VGRF have also been limited. Thus, in this study, we focused on the vertical ground force component, classified into 2 groups: M-shaped, also known as a "dual-hump" shape (18) and non-M-shaped. The purpose of this study was to evaluate the relationship between knee pain and various indicators of the combined performance of the leg, including gait parameters, functional performance, TUG and FR and to determine whether the classification of VGRF is correlated with gait parameters and functional performance.

## MATERIAL AND METHODS

### *Subjects*

We defined the subjects with osteoarthritic knee as having knee pain and less than 100 points of Japan Orthopaedic Association (JOA) score. We have been performing annual medical checks of adults aged 65 years and

 *ISSN 1650–1977*
DOI 10.1080/16501970310018297

Table I. *Japan Orthopaedic Association scores based on the osteoarthritic knee evaluation form*

| *Pain on walking (maximum 30 points)* | *Score* |
|---|---|
| No pain, walking unlimited | 30 |
| Pain, walking unlimited | 25 |
| Pain, walking distance of 0.5–1 km | 20 |
| Pain, walking less than 0.5 km | 15 |
| Pain, walking only indoors | 10 |
| Cannot walk | 5 |
| Cannot stand | 0 |
| *Pain on ascending or descending stairs (maximum 25 points)* | |
| No pain | 25 |
| Pain, relieved by using handrails | 20 |
| Pain, with handrails, but no pain with each step | 15 |
| Pain, with each step, pain relieved by using handrails | 10 |
| Pain, with each step even with handrail use | 5 |
| Cannot ascend or descend | 0 |
| *Range of motion (maximum 35 points)* | |
| Kneeling | 35 |
| Sideways or cross-legged sitting | 30 |
| More than 110° | 25 |
| 75°–109° | 20 |
| 35°–74° | 10 |
| Less than 35° | 0 |
| *Joint effusion (maximum 10 points)* | |
| No effusion | 10 |
| Occasional puncture required | 5 |
| Frequent puncture required | 0 |
| Maximum total points | 100 |

over who live in the community in Kahoku of Kochi prefecture since 1994. We then examined the locomotor ability of the subjects.

The mean age of the 130 participants was 80 years (range 65–94 years), with a mean height of 143.0 cm. Knee pain while walking was classified into 3 groups: no pain (45%), unilateral pain (28%) or bilateral pain (26%).

Average maximum flexion for all subjects was 140.9 ± 13.4 degrees. Average maximum extension was 5.2 ± 6.1 degrees. JOA scores determined from the osteoarthritic knee evaluation form (Table I) were used for the evaluation of knee function (19). JOA (0–100 points) scores averaged 90.1 ± 12.9 points. The distance between the medial chondyles was evaluated, and averaged 2.5 ± 1.4 fingers breadth.

Co-morbidities of the subjects included hypertension (31.6%), cardiac arrhythmia (6.1%), coronary artery disease (3.2%) and diabetes mellitus (5.7%). Eighteen subjects with the following conditions were excluded from this study: knee disorders after total knee arthroplasty (5 patients), high tibial osteotomy (2 patients), miscellaneous knee operations (2 patients), osteosynthesis (1 patient), multiple cerebral infarctions (7 patients) and Parkinson's disease (1 patient).

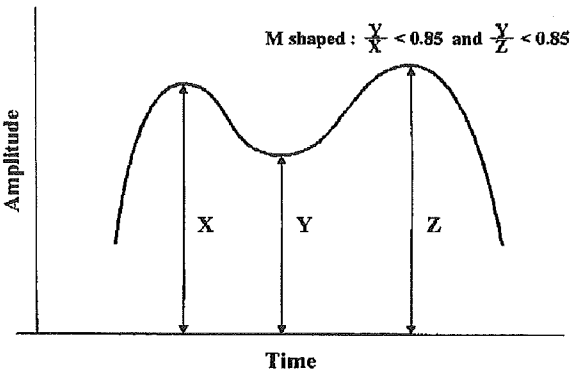


*Fig. 1.* Calculation of M-wave shape of vertical ground reaction force. M-shaped was defined as Y/X and Y/Z less than 0.85. All others were defined as non-M-shaped.

*Gait analysis*

The interviewer asked to record the gait parameters of subjects who were able to walk a distance of 10 metres. Subjects were allowed to wear their usual clothes and use their preferred (normal) speed while walking a 7-metre-long course. The first and last 2–3 metres on the walkway were not considered for measurement.

A Gait Scan® 8000 (Nitta Co. Ltd, Osaka, Japan) of gait-pattern measurement system consisting of a thin-film sensor walkway, a computer for automatic recording of the data was used in this study. This gait analysis device consists of a sensor seat (264 × 52 cm), a connector unit which fixes the sensor seat, and an interface board with a personal computer and software for data analysis.

Gait parameters, temporal distance and time factors, and ground reaction forces were measured simultaneously. Ground reaction force data for both legs was collected at a self-selected walking speed. The peak force was measured as the highest VGRF that occurred anytime during the stance phase, while the lowest VGRF occurred during the mid-stance phase.

Patients were classified into 2 groups based on the VGRF: M-shaped and non-M-shaped (Fig. 1). We defined M-shaped as lowest/highest × 100 (%) of less than 85. We assessed the shape of the VGRF for every step and classified individuals based on the result that was obtained for the greater number of steps. The mean gait variables measured in this study were walking speed (metres/sec), stride length, step width (cm), time of stride, time of single stance and time of double stance (sec). The distance parameters of stride length and step width were normalized for the height of the subject (15).

*Functional performance*

*Timed up and go*

To measure TUG, subjects were given oral instructions to stand up from

Table II. *Data (mean (SD)) for patients without pain, with unilateral and bilateral pain in elderly females*

| | No pain ($n = 59$) | Unilateral pain ($n = 37$) | Bilateral pain ($n = 34$) |
|---|---|---|---|
| Body weight (kg) | 45.2 (7.53) | 47.2 (7.49) | 52.2 (8.94) |
| Timed up and go (sec) | 13.0 (3.0) | 13.8 (4.51) | 15.1 (7.28) |
| Functional reach (cm) | 20.6 (7.2) | 21.0 (7.07) | 23.1 (6.89) |
| Stride length (cm) | 63.2 (9.21) | 61.1 (11.7) | 61.7 (10.9) |
| Stride width (cm) | 5.4 (2.20) | 5.7 (2.14) | 5.6 (1.92) |
| Time of stride (sec) | 1.1 (0.117) | 1.1 (0.179) | 1.2 (0.167) |
| Time of single stance (sec) | 0.58 (0.059) | 0.59 (0.073) | 0.60 (0.082) |
| Time of double stance (sec) | 0.16 (0.037) | 0.17 (0.052) | 0.18 (0.069) |
| Gait speed (m/s) | 0.6 (0.115) | 0.56 (0.147) | 0.54 (0.135) |

Table III. *Participant characteristics given as mean (SD)*

| | Height (cm) | Weight (kg) | JOA (point) | TUG (sec) | FR (cm) |
|---|---|---|---|---|---|
| Right side | | | | | |
| M-shaped ($n=32$) | 143.8 (7.2) | 46.1 (8.6) | 95.2 (10.3) | 11.6 (2.3) | 22.5 (6.9) |
| Non-M-shaped ($n=47$) | 142.4 (5.2) | 45.9 (7.4) | 86.6 (13.5) | 14.6 (4.5) | 18.4 (8.2) |
| | $p=0.187$ | $p=0.96$ | $p=0.0013$ | $p<0.0001$ | $p=0.026$ |
| Left side | | | | | |
| M-shaped ($n=29$) | 143.1 (8.1) | 45.8 (8.1) | 96.9 (6.25) | 11.35 (2.25) | 22.9 (7.56) |
| Non-M-shaped ($n=50$) | 142.9 (4.7) | 46.2 (7.8) | 86.1 (14.1) | 14.5 (4.44) | 18.45 (7.74) |
| | $p=0.41$ | $p=0.92$ | $p=0.0002$ | $p<0.0001$ | $p=0.026$ |

JOA: Japan Orthopaedic Association; TUG: timed up and go; FR: functional reach

a chair, walk 3 metres as quickly and as safely as possible, cross a line marked on the floor, turn around, walk back and sit down (6).

*Functional reach.* FR represents the maximal distance a subject can reach forward beyond arm's length while maintaining a fixed base of support in the standing position (7, 20).

*Statistics*

Data were expressed as a mean and standard deviation (SD). Differences between groups were evaluated using a Kruskal Wallis test for the analysis of knee pain (Table II) and a Mann-Whitney U test for the analysis of VGRF (Tables III and IV). Statistical significance was set at $p<0.05$.

## RESULTS

Occurrence of knee pain showed a significant association with body weight; however, there was no significant difference between patients with or without pain and TUG, FR, or any gait parameters (Table II).

The shape of the VGRF was associated with certain measures of functional performance, as well as the JOA score (Table III). Patients exhibiting an M-shaped VGRF on the right and left sides had shorter TUGs and longer FRs than patients with a non-M-shaped VGRF. The total JOA score was greater for the M-shaped group than for the non-M-shaped group. Within both groups, the ground reaction forces were similar on left and right sides.

Several gait parameters varied according to the shape of the VGRF (Table IV). Stride length was longer for the M-shaped VGFR group than for the non-M-shaped VGRF group. The times of stride and single and double stance were shorter in the M-shaped VGRF group than in the non-M-shaped group. The walking speed of the M-shaped group was faster than that of the non-M-shaped group. There was no significant difference between the 2 groups in the step width on both sides.

## DISCUSSION

Osteoarthritis of the knee is common in elderly females and it is well-known that it is associated with gait disturbances. There have been numerous reports regarding the relationship between osteoarthritis and gait parameters. An evaluation of the relationship between gait parameters and knee pain in elderly females found no significant association between knee pain and gait parameters or functional performance. Findings such as these have suggested that numerous factors, such as the posture of the trunk, lumbar lesions, the condition of other joints (such as the hip and ankle) and mental status, all contribute to gait parameters in elderly females. Therefore, it is important to consider these factors in the analysis of people with knee pain.

An advantage of gait analysis as a diagnostic or research tool is that many factors can be assessed at one time; however, proper evaluation of the resulting data can be complex. Quantitative data of time and distance parameters of gait analysis is difficult to understand and interpret whether it is within normal or not.

One study showed no overall abnormality in the shape or amplitude of the ground reaction force measured for the natural gait of knee-pain subjects (21). The present study, which involved the evaluation of one simple aspect of the VGRF (classified as M-shaped and non-M-shaped), showed that the shape of the ground reaction force was correlated with the pain

Table IV. *Gait parameters (mean (SD)) for subjects with M-shape and non-M-shape of vertical ground reaction force*

| | Stride length (cm) | Step width (cm) | Time of stride (sec) | Time of single stance (sec) | Time of double stance (sec) | Gait speed (m/s) |
|---|---|---|---|---|---|---|
| Right side | | | | | | |
| M-shaped ($n=32$) | 70.1 (8.7) | 5.5 (2.1) | 1.03 (0.09) | 0.5 (0.04) | 0.1 (0.02) | 0.7 (0.11) |
| Non-M-shaped ($n=47$) | 55.8 (89.9) | 5.8 (2.3) | 1.2 (0.15) | 0.6 (0.07) | 0.2 (0.047) | 0.5 (0.1) |
| | $p<0.0001$ | $p=0.712$ | $p<0.0001$ | $p<0.0001$ | $p<0.0001$ | $p<0.0001$ |
| Left side | | | | | | |
| M-shaped ($n=29$) | 70.6 (9.2) | 5.5 (2.08) | 1.0 (0.087) | 0.54 (0.042) | 0.1 (0.02) | 0.69 (0.12) |
| Non-M-shaped ($n=50$) | 56.5 (9.9) | 6.0 (2.47) | 1.8 (0.15) | 0.61 (0.075) | 0.2 (0.046) | 0.5 (0.11) |
| | $p<0.0001$ | $p=0.146$ | $p<0.0001$ | $p<0.0001$ | $p<0.0001$ | $p<0.0001$ |

component of the JOA score. In another study, increased gait speed was associated with shorter force periods and larger peak forces (16).

In the present study we found that there were no differences between the right and left legs with respect to gait parameters, functional performance or the shape of the ground reaction force. Consistent with our findings, another study showed no significant differences between the right and left foot with respect to ground reaction force during walking (22).

In our study we found that both gait parameters and functional performance were significantly correlated with the shape of the VGRF. Several previous studies have examined VGRFs in normal subjects and patients with osteoarthritis; however, prior to the present study, there was little known concerning the relationship between the VGRF and gait parameters or functional performance in elderly females with knee osteoarthritis. In one study it was found that the 2 peaks in the vertical component measured for the affected side in knee-osteoarthritis patients became less apparent, with significantly lower magnitudes than in normal subjects (18). In addition, patterns of VGRFs were nearly identical during overground and treadmill walking (23) and the general waveform and its characteristic features did not seem to be affected by the sex of normal subjects (18). In the present study, we could not find a correlation between pain and the mechanism of the shape of VGRF. Further study is needed to clarify the changing mechanism of VGRF in osteoarthritic knee.

In the present study, we did not examine inter-rater reliability: future study is needed to investigate this and the validity with respect to M-shape and gait analysis.

In conclusion, our classification of VGRF is a simple and useful tool for assessment of gait function. It was correlated with many parameters of gait and functional performance, such as TUG and functional reach. Our study indicated that a change in the VGRF, from non-M-shaped to M-shaped, is crucial to the improvement of gait parameters and gait performance. Further studies are needed to seek methods for altering the shape of the ground reaction force.

## ACKNOWLEDGEMENTS

We thank all staff members and elderly residents of Kahoku in Kochi prefecture who were involved in this study.

## REFERENCES

1. Murray MP, Gore DR, Sepic SB, Mollinger LA. Antalgic maneuvers during walking in men with unilateral knee disability. Clin Orthop 1985; 199: 192–200.
2. Prince F, Corriveau H, Hebert R, Winter DA. Gait in the elderly. Gait Posture 1997; 5: 128–135.
3. Stauffer RN, Chao EYS, Gyory AN. Biomechanical gait analysis of the diseased knee joint. Clin Orthop 1977; 126: 246–255.
4. Kaufman KR, Sutherland DH. Future trends in human motion analysis. In: Harris GF, Smith PA, eds. Human motion analysis. Current applications and future directions. New York: IEEE Press; 1996, p. 187–215.
5. Bertani A, Cappello A, Benedetti MG, Simoncini L, Catani F. Flat foot functional evaluation using pattern recognition of ground reaction data. Clin Biomech 1999; 14: 484–493.
6. Podsiadlo D, Richardson S. The timed "Up & Go": a test of basic functional mobility for frail elderly persons. J Am Geriatr Soc 1991; 39: 142–148.
7. Duncan PW, Weiner DK, Chandler J, Studenski S. Functional reach: a new clinical measure of balance. J Gerontol 1990; 45: 192–197.
8. Weiner DK, Duncan PW, Chandler J, Studenski SA. Functional reach: a marker of physical frailty. J Am Geriatr Soc 1992; 40: 203–207.
9. Goh JC, Bose K, Khoo BC. Gait analysis study on patients with varus osteoarthritis of the knee. Clin Orthop 1993; 294: 223–231.
10. Kadaba MP, Ramakrishnan HK, Wootten ME, Gainey J, Gorton G, Cochran GVB. Repeatability of kinematic, kinetic, and electromyographic data in normal adult gait. J Orthop Res 1989; 7: 849–860.
11. Olsson E, Oberg K, Ribbe T. A computerized method for clinical gait analysis of floor reaction forces and joint angular motion. Scand J Rehabil Med 1986; 18: 93–99.
12. Andriacchi TP, Ogle JA, Galante JO. Walking speed as a basis for abnormal gait measurements. J Biomech 1977; 10: 261–268.
13. Alexander RM, Jayes AS. Fourier analysis of forces exerted in walking and running. J Biomech 1980; 13: 383–390.
14. Balmaseda MT, Koozekanani SH, Fatehi MT, Gordon C, Dreyfuss PH, Tanbonlinog EC. Ground reaction forces, center of pressure, and duration of stance with and without an ankle-foot orthosis. Arch Phys Med Rehabil 1988; 69: 1009–1112.
15. Chao EY, Laughman RK, Schneider E, Stauffer RN. Normative data of knee joint motion and ground reaction forces in adult level walking. J Biomech 1983; 16: 219–233.
16. Nilsson J, Thorstensson A. Ground reaction forces at different speeds of human walking and running. Acta Physiol Scand 1989; 136: 217–227.
17. Cook TM, Farrell KP, Carey IA, Gibbs JM, Wiger GE. Effects of restricted knee flexion and walking speed on the vertical ground reaction force during gait. J Orthop Sports Phy Ther 1997; 25: 236–244.
18. Schneider E, Chao EY. Fourier analysis of ground reaction forces in normals and patients with knee joint disease. J Biomech 1983; 16: 591–601.
19. Takahashi T, Wada Y, Tanaka M, Iwagawa M, Ikeuchi M, Hirose D, Yamamoto H. Dome-shaped proximal tibial osteotomy using percutaneous drilling for osteoarthritis of the knee. Arch Orthop Trauma Surg 2000; 120: 32–37.
20. Okumiya K, Matsubayashi K, Wada T, Kimura S, Doi Y, Ozawa T. Effects of exercise on neurobehavioral function in community-dwelling older people more than 75 years of age. J Am Geriatr Soc 1996; 44: 569–572.
21. Radin EL, Yang KH, Riegger C, Kish VL, O'Connor JJ. Relationship between lower limb dynamics and knee joint pain. J Orthop Res 1991; 9: 398–405.
22. Herzog W, Nigg BM, Read LJ, Olsson E. Asymmetries in ground reaction force patterns in normal human gait. Med Sci Sports Exerc 1989; 21: 110–114.
23. White SC, Yack HJ, Tucker CA, Lin HY. Comparison of vertical ground reaction forces during overground and treadmill walking. Med Sci Sports Exerc 1998; 30: 1537–1542.

Oncogene (2005), 1–10

www.nature.com/onc

ORIGINAL ARTICLE

# Sirt1 inhibitor, Sirtinol, induces senescence-like growth arrest with attenuated Ras–MAPK signaling in human cancer cells

H Ota[1,2], E Tokunaga[1,3], K Chang[1], M Hikasa[1], K Iijima[2], M Eto[2], K Kozaki[2], M Akishita[2], Y Ouchi[2] and M Kaneki[1,3]

*[1]Department of Anesthesia & Critical Care, Massachusetts General Hospital, Harvard Medical School, Charlestown, MA, USA; [2]Department of Geriatric Medicine, Graduate School of Medicine, University of Tokyo, Bunkyo, Tokyo, Japan and [3]Shriners Hospital for Children, Boston, MA, USA*

**The induction of senescence-like growth arrest has emerged as a putative contributor to the anticancer effects of chemotherapeutic agents. Clinical trials are underway to evaluate the efficacy of inhibitors for class I and II histone deacetylases to treat malignancies. However, a potential antiproliferative effect of inhibitor for Sirt1, which is an NAD$^+$-dependent deacetylase and belongs to class III histone deacetylases, has not yet been explored. Here, we show that Sirt1 inhibitor, Sirtinol, induced senescence-like growth arrest characterized by induction of senescence-associated β-galactosidase activity and increased expression of plasminogen activator inhibitor 1 in human breast cancer MCF-7 cells and lung cancer H1299 cells. Sirtinol-induced senescence-like growth arrest was accompanied by impaired activation of mitogen-activated protein kinase (MAPK) pathways, namely, extracellular-regulated protein kinase, c-*jun* N-terminal kinase and p38 MAPK, in response to epidermal growth factor (EGF) and insulin-like growth factor-I (IGF-I). Active Ras was reduced in Sirtinol-treated senescent cells compared with untreated cells. However, tyrosine phosphorylation of the receptors for EGF and IGF-I and Akt/PKB activation were unaltered by Sirtinol treatment. These results suggest that inhibitors for Sirt1 may have anticancer potential, and that impaired activation of Ras–MAPK pathway might take part in a senescence-like growth arrest program induced by Sirtinol.**
*Oncogene* advance online publication, 19 September 2005; doi:10.1038/sj.onc.1209049

**Keywords:** Sirt1; Sirtinol; cellular senescence; Ras; MAPK; Akt/PKB

## Introduction

Cellular senescence is a state with permanent loss of replicative capability even upon mitogenic stimuli. Cellular senescence is characterized by phenotypic alterations including induction of senescence-associated β-galactosidase (SA-β-gal), a large and flat cell morphology and increased expression of plasminogen activator inhibitor 1 (PAI-1) (Goldstein *et al.*, 1994; Dimri *et al.*, 1995).

Immortalization, an escape from the replicative senescence program, is a necessary step for neoplastic transformation of cells. Hence, transformed cells can bypass the replicative senescence program. However, cancer and leukemia cells still retain the capacity to undergo premature senescence in response to various stimuli. Senescent normal human fibroblasts usually exhibit G1 cell cycle arrest. However, polyploidy and multinucleation are also associated with replicative senescence and premature senescence in various cell types, including human normal endothelial cells (Aviv *et al.*, 2001; Wagner *et al.*, 2001) and breast cancer MCF-7 cells (Kim *et al.*, 2003).

Anticancer chemotherapeutic agents and ionizing radiation have been shown to cause senescence-like growth arrest in human cancer cells *in vitro* and *in vivo* (Han *et al.*, 2002; Schmitt *et al.*, 2002; te Poele *et al.*, 2002; Shay and Roninson, 2004). Induction of SA-β-gal staining by chemotherapy was observed *in vivo* in cancer and lymphoma cells in rodents (Elmore *et al.*, 2002; Roninson, 2002; Schmitt *et al.*, 2002; Christov *et al.*, 2003) and in patients with breast cancer (te Poele *et al.*, 2002). Thus, senescence-like growth arrest has been proposed to be a putative determinant of *in vivo* tumor response to chemotherapeutic agents and ionizing radiation (Mathon and Lloyd, 2001; Wang *et al.*, 2003; Ben-Porath and Weinberg, 2004; Kahlem *et al.*, 2004; Pelicci, 2004; Sharpless and DePinho, 2004; Shay and Roninson, 2004).

Sirt1 is a mammalian NAD$^+$-dependent deacetylase that belongs to class III histone deacetylases (HDACs) (Imai *et al.*, 2000; Landry *et al.*, 2000; Blander and Guarente, 2004). Sir2, yeast homologue of Sirt1, is involved in a number of cellular processes including gene silencing at telomere and mating loci, DNA repair, recombination and aging. Recent studies demonstrated that Sirt1 plays an important role in the regulation of cell fate and stress response in mammalian cells. Sirt1 promotes cell survival by inhibiting apoptosis or cellular senescence induced by stresses including DNA damage

Correspondence: Dr M Kaneki, Department of Anesthesia & Critical Care, Massachusetts General Hospital, Harvard Medical School, 149 Thirteenth Street, Rm 6604, Charlestown, MA 02129, USA.
E-mail: mkaneki@partners.org
Received 23 June 2005; accepted 8 July 2005

and oxidative stress. An increasing number of proteins have been identified as substrates of Sirt1, including p53 (Luo *et al.*, 2001; Vaziri *et al.*, 2001; Langley *et al.*, 2002), FOXO transcription factors (Brunet *et al.*, 2004; Daitoku *et al.*, 2004; Motta *et al.*, 2004; van der Horst *et al.*, 2004), peroxisome proliferator-activated receptor-$\gamma$ (Picard *et al.*, 2004) and Ku70 (Cohen *et al.*, 2004).

Sirt1 deacetylase, a member of the class III HDAC family, exhibits distinct biochemical characteristics from conventional class I and class II HDACs. Inhibitors for class I and class II HDACs, such as trichostatin A and its derivatives, do not inhibit the deacetylating activity of Sirt1 (Imai *et al.*, 2000). Conversely, specific inhibitors for Sirt1 such as Sirtinol do not inhibit class I and class II HDACs, either (Bedalov *et al.*, 2001; Grozinger *et al.*, 2001).

Class I and class II HDAC inhibitors exhibit antiproliferative effects in human cancer cells (Rosato and Grant, 2004; Vanhaecke *et al.*, 2004; Vigushin and Coombes, 2004). The efficacy of class I and class II HDAC inhibitors for treatment of patients with cancer or leukemia has been examined in phase I and II clinical trials (Piekarz *et al.*, 2001; Sandor *et al.*, 2002; Kelly *et al.*, 2003; McLaughlin and La Thangue, 2004; Piekarz and Bates, 2004). However, the effects of inhibitor for Sirt1 or class III HDACs on cell growth have not yet been investigated. Here, we show that Sirtinol, a specific inhibitor for Sirt1, induced senescence-like growth arrest in human breast cancer MCF-7 and lung cancer H1299 cells, and that Sirtinol-induced senescence-like growth arrest was accompanied by blunted activation of Ras–mitogen-activated protein kinase (MAPK) pathways in response to growth factors.

## Results

### *Sirtinol, Sirt1 inhibitor, induced senescence-like growth arrest in human MCF-7 and H1299 cells*

MCF-7 and H1299 cells were exposed to Sirtinol (100 $\mu$M) for 24 h; then Sirtinol was removed from the culture media. Treatment with Sirtinol inhibited cell growth in both MCF-7 and H1299 cells (Figure 1a and b). The inhibition of cell growth was persistent and observed up to 9 days after Sirtinol withdrawal. These results suggest that Sirtinol caused a sustained growth arrest. This was supported by reduced incorporation of BrdU in Sirtinol-treated MCF-7 and H1299 cells at 10 days after the addition of Sirtinol, as compared with untreated cells (Figure 1c and d).

We examined the effects of Sirtinol treatment on SA-$\beta$-gal activity and the expression of PAI-1, characteristic features of senescence-like growth arrest. Sirtinol treatment increased SA-$\beta$-gal-positive cells in a dose-dependent manner 10 days after the addition of Sirtinol in both MCF-7 and H1299 cells (Figures 2 and 3a), but the extent of SA-$\beta$-gal induction was relatively smaller in H1299 than in MCF-7 cells. Only a small number of MCF-7 and H1299 cells were SA-$\beta$-gal-positive when untreated. Enlarged, flattened morphology was

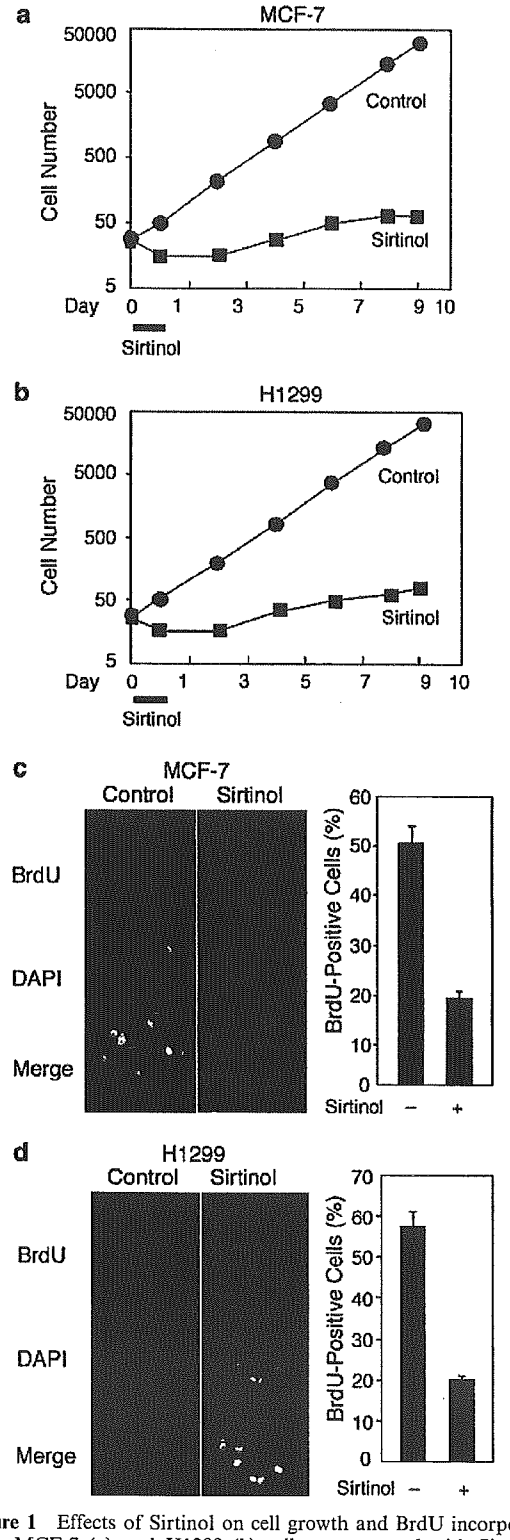


**Figure 1** Effects of Sirtinol on cell growth and BrdU incorporation. MCF-7 (**a**) and H1299 (**b**) cells were treated with Sirtinol (100 $\mu$M) for 24 h. At 24 h after the addition of Sirtinol, Sirtinol was removed from the media, and then the cells were cultured in inhibitor-free complete media. (**c**, **d**) BrdU incorporation was evaluated at 10 days after the addition of Sirtinol (100 $\mu$M). BrdU incorporation was decreased in Sirtinol-treated MCF-7 (**c**) and H1299 (**d**) cells compared with untreated cells (Control).

observed in Sirtinol-treated MCF-7 cells and, to a lesser extent, in Sirtinol-treated H1299 cells, as compared with untreated cells. Sirtinol treatment also resulted in increased expression of PAI-1 in both MCF-7 and H1299 cells (Figure 3b). β-Actin expression, however, was not affected by Sirtinol.

Treatment with Splitomicin, another specific inhibitor for Sirt1, for 24 h also led to the induction of SA-β-gal staining in a dose-dependent manner (Figure 3a). However, greater concentrations of Splitomicin appeared to be required to induce SA-β-gal, as compared with Sirtinol.

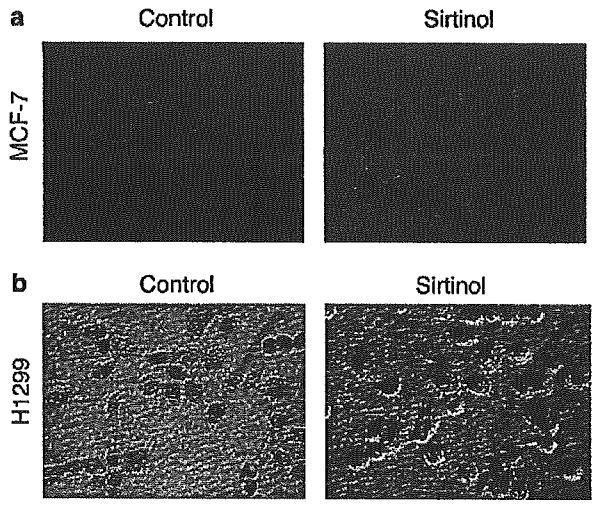


**Figure 2** SA-β-gal staining in Sirtinol-treated cells. At 10 days after the addition of Sirtinol (100 μM), MCF-7 (**a**) and H1299 (**b**) cells were stained for SA-β-gal. Sirtinol treatment increased SA-β-gal-positive cells in MCF-7 and H1299 cells. In addition, the number of multinucleated cells was increased in Sirtinol-treated MCF-7 cells, but not in Sirtinol-treated H1299 cells, compared with untreated (Control) cells. Arrowheads denote multinucleated cells in Sirtinol-treated MCF-7 cells.

Colony formation assay also revealed that both Sirtinol and Splitomicin elicited antiproliferative effects in MCF-7 and H1299 cells in a dose-dependent manner (Figure 4). Sirtinol inhibited colony formation at concentrations of 33 μM and higher in MCF-7 and H1299 cells. On the other hand, 33 μM Splitomicin failed to decrease the number of colonies, but Splitomicin at 100 and 333 μM effectively inhibited colony formation in MCF-7 and H1299 cells.

Senescence-like growth arrest by Sirt1 inhibition was further corroborated by experiments using short interfering RNA (siRNA). Gene knockdown of Sirt1 by siRNA resulted in induction of SA-β-gal staining, large and flat cell morphology, decreased BrdU incorporation and increased PAI-1 expression in both MCF-7 and H1299 cells, as compared with control siRNA (Figure 5). Moreover, Sirt1 inhibition by Sirtinol, Splitomicin or siRNA also induced senescence-like phenotype in human diploid fibroblasts, WI-38 and IMR-90 cells, reflected by induction of SA-β-gal staining, and enlarged and flattened cell morphology (Supplementary Figure 1).

In Sirtinol-treated MCF-7 cells, the number of multinucleated cells was increased compared with untreated cells (Figure 2), but multinucleated cells were not found in H1299 cells regardless of whether treated with or without Sirtinol. Consistent with these observations, flow cytometric analysis revealed that the substantial cell population of Sirtinol-treated MCF-7 cells exhibited DNA content over 4*N*, indicative of polyploidy (Figure 6a). Polyploidy fraction estimated by the ratio

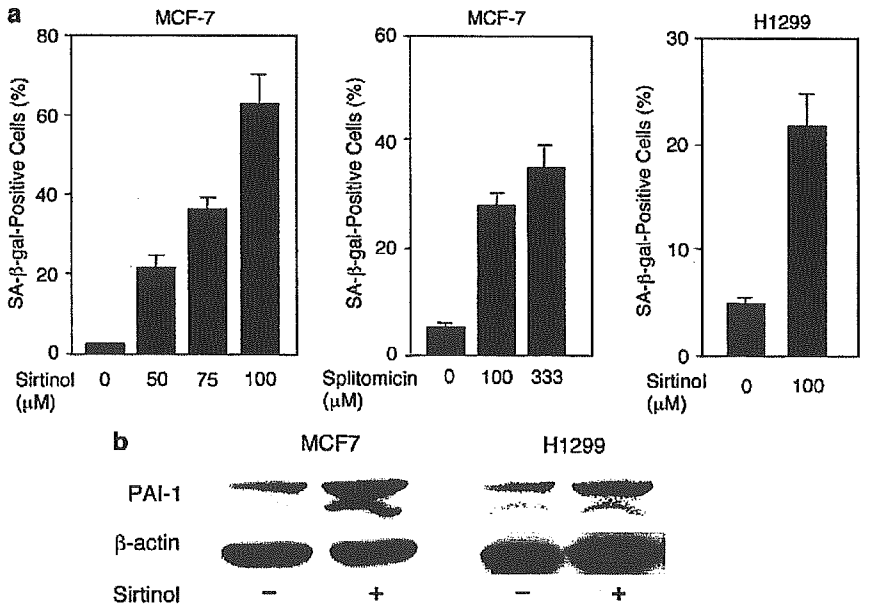


**Figure 3** Effects of Sirtinol and Splitomicin on SA-β-gal activity and PAI-1 expression. (**a**) SA-β-gal-positive cells were counted 10 days after the addition of indicated concentrations of Sirtinol or Splitomicin in MCF-7 and H1299 cells. Treatment with Sirtinol and Splitomicin increased SA-β-gal-positive cells in a dose-dependent manner. (**b**) Sirtinol treatment resulted in the increased expression of PAI-1 as compared with untreated cells.

of cell population with DNA content of over $4N$ to that with over $2N$ was greater in Sirtinol-treated MCF-7 cells than in untreated cells (Figure 6a, right panel). In contrast, Sirtinol-treated H1299 cells were cell cycle arrested at G1 (Figure 6b). There was little, if any, increase in polyploidy fraction by Sirtinol in H1299 cells (control: 0.6%; Sirtinol: 1.6%).

In cellular senescence, induction of p53, dephosphorylation of Rb and increased expression of cyclin-dependent kinase inhibitors such as p16, p21 and p27 have been shown to be involved (Serrano *et al.*, 1997; Collado *et al.*, 2000; Alexander and Hinds, 2001; Beausejour *et al.*, 2003; Jirawatnotai *et al.*, 2003; Mallette *et al.*, 2004). We found that phosphorylated Rb was decreased in Sirtinol-treated MCF-7 and H1299 cells compared with untreated cells, while the protein expression of Rb was unaltered (Figure 7a and b). p27 expression was induced in Sirtinol-treated MCF-7 and H1299 cells (Figure 7f and g), while β-actin expression was unaltered. However, the mRNA level of p27 was not increased by Sirtinol treatment in MCF-7 and H1299 cells at both 3 and 10 days after the addition of Sirtinol, while tamoxifen and serum starvation upregulated the p27 mRNA level in MCF-7 and H1299 cells, respectively (Supplementary Figure 2). In contrast, p21 was not increased in Sirtinol-treated MCF-7 and H1299 cells compared with untreated cells. p16 was not induced in Sirtinol-treated H1299 cells (Figure 7g). MCF-7 and H1299 cells are deficient in p16 and p53, respectively. On the other hand, treatment with tamoxifen (1 μM) for 24 h increased protein expression of p21 and p27 in MCF-7 cells, and serum starvation for 24 h induced p16, p21 and p27 expression in H1299 cells. Neither expression nor acetylation of p53 was upregulated by Sirtinol

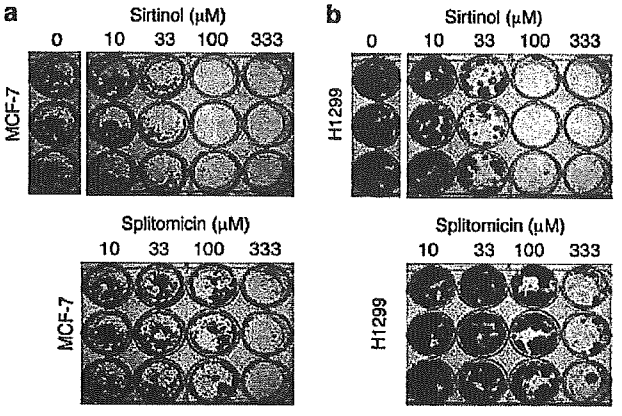


**Figure 4** The effects of Sirtinol and Splitomicin on colony formation. MCF-7 (**a**) and H1299 (**b**) cells were inoculated onto 12-well plates at the density of 500 cells/well, and treated with the indicated concentrations of Sirtinol or Splitomicin for 24 h. After withdrawal of the Sirt1 inhibitors, the cells were cultured for 14 days. Both Sirtinol and Splitomicin inhibited colony formation in a dose-dependent manner.

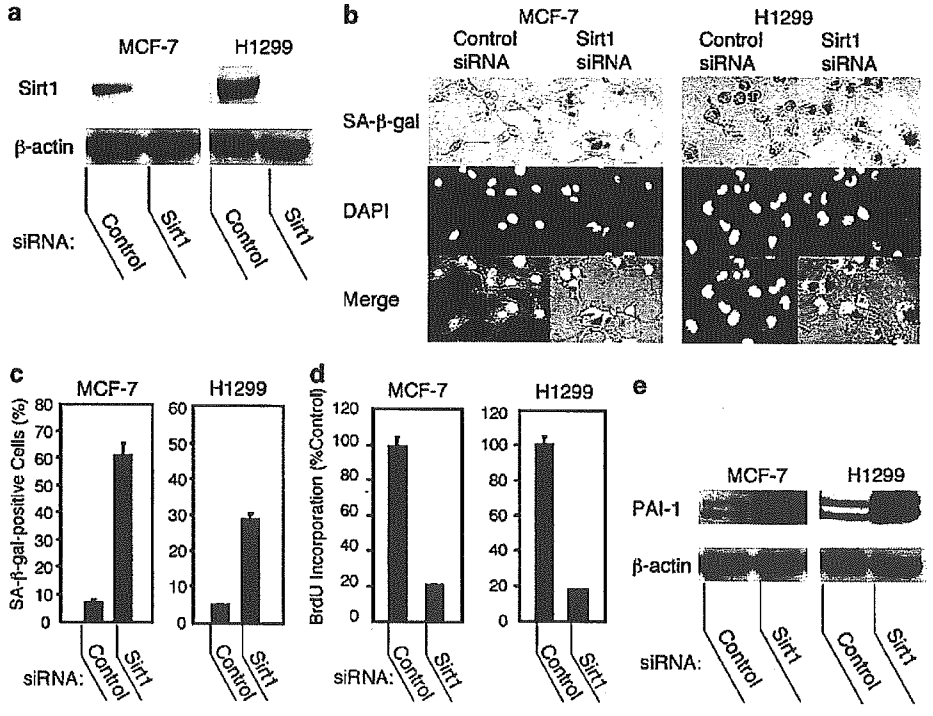


**Figure 5** Gene knockdown of Sirt1 by siRNA induced senescence-like phenotype. MCF-7 and H1299 cells were treated with siRNA for Sirt1 or control siRNA. (**a**) At 3 days after the transfection, immunoblot analysis revealed that Sirt1 siRNA effectively reduced Sirt1 expression in both MCF-7 and H1299 cells. (**b**, **c**) At 10 days after the transfection, SA-β-gal-positive cells were significantly increased in Sirt1 siRNA-treated cells compared with control siRNA-treated cells. (**d**) BrdU incorporation was decreased in Sirt1 siRNA-treated cells compared with control siRNA-treated cells at 10 days after the transfection. (**e**) Sirt1 siRNA increased PAI-1 protein expression compared with control siRNA at 10 days after the transfection.

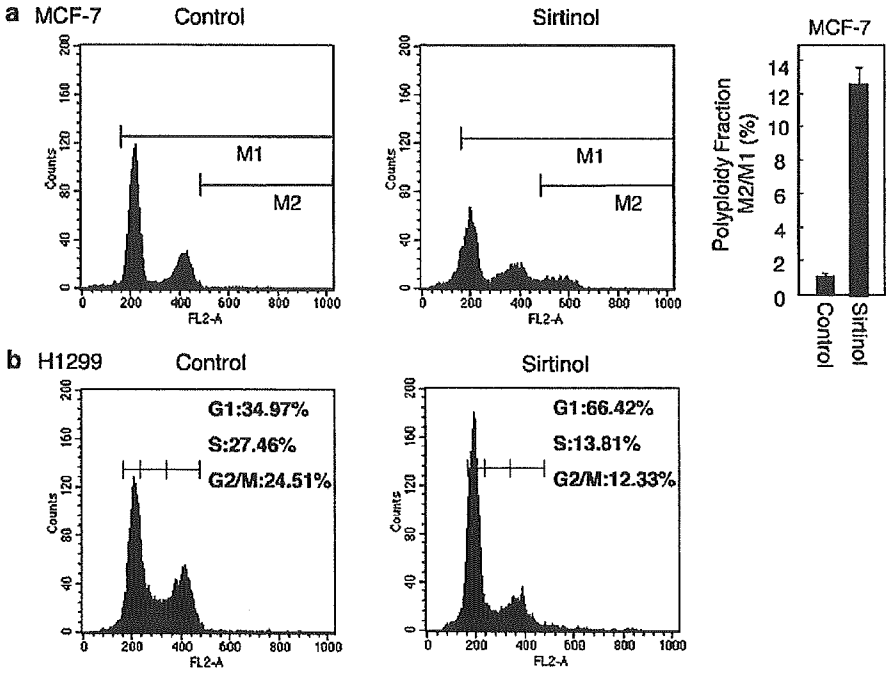


**Figure 6** Flow cytometric analysis of Sirtinol-treated cells. At 10 days after the addition of Sirtinol (100 $\mu$M), the cell cycle of MCF-7 (**a**) and H1299 (**b**) cells was analysed by flow cytometry. In Sirtinol-treated MCF-7 cells, polyploidy fraction (M2/M1; cell population with DNA content of over 4*N* normalized to that with DNA content of over 2*N*) was increased compared with untreated MCF-7 cells (Control). Sirtinol-treated H1299 cells exhibited G1 cell cycle arrest (**b**).

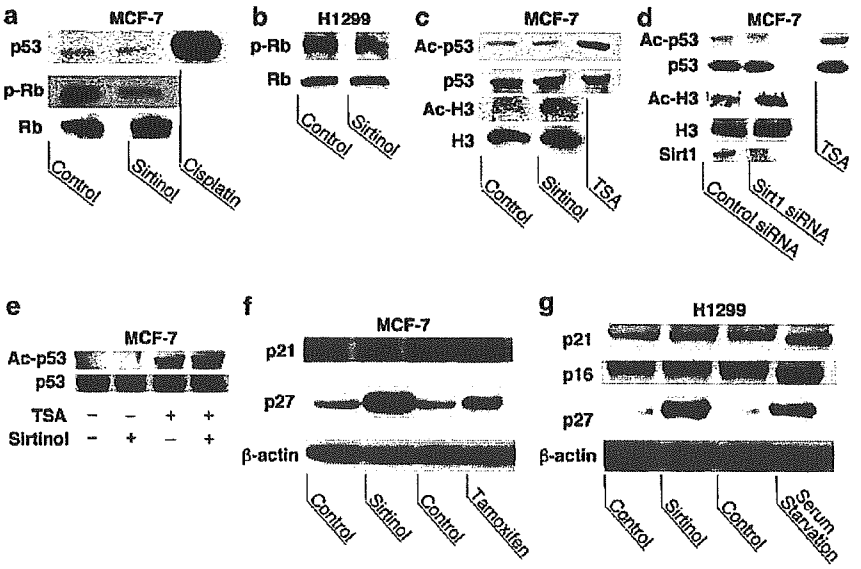


**Figure 7** p53, Rb and cyclin-dependent kinase inhibitors in Sirtinol-treated cells. (**a**, **b**) At 10 days after the addition of Sirtinol (100 $\mu$M), phosphorylated Rb (p-Rb) was decreased in Sirtinol-treated MCF-7 and H1299 cells compared with untreated cells. (**a**, **c**, **d**) The expression and acetylation of p53 were not increased by Sirtinol (**a**, **c**) or siRNA for Sirt1 (**d**) in MCF-7 cells. However, a robust increase in expression and acetylation of p53 (Ac-p53) were found in MCF-7 cells when treated with cisplatin (40 $\mu$M) for 18 h and trichostatin A (TSA, 5 $\mu$M) for 4 h, respectively. In contrast, Sirtinol (100 $\mu$M) treatment and siRNA for Sirt1 increased acetylated histone H3 (Ac-H3), while the abundance of histone H3 was unaltered (**c**, **d**). (**e**) MCF-7 cells were treated with or without Sirtinol (100 $\mu$M) in the presence or absence of trichostatin A (TSA, 0.5 $\mu$M) for 24 h. Sirtinol enhanced trichostatin A-induced acetylation of p53. p53 expression was not altered by Sirtinol or trichostatin A. (**f**, **g**) p21 expression was not increased by Sirtinol treatment in MCF-7 and H1299 cells. p16 expression was not induced by Sirtinol treatment in H1299 cells. In contrast, the expression of p27 was increased in Sirtinol-treated MCF-7 and H1299 cells compared with untreated cells.

or siRNA for Sirt1 in MCF-7 cells that harbor wild-type p53 (Figure 7c and d), while acetylation of histone H3 was increased by Sirtinol and siRNA for Sirt1. However, cisplatin and trichostatin A, class I and class II HDAC inhibitor, caused robust induction of p53 and acetylation of p53 in MCF-7 cells, respectively (Figure 7a and c–e). Although Sirtinol alone did not increase p53 acetylation, Sirtinol enhanced p53 acetylation in the presence of trichostatin A (Figure 7e). These results are consistent with previous observations that inhibition of Sirt1 by itself did not induce p53 acetylation in the absence of other stimulus, while DNA damage- or oxidative stress-induced p53 acetylation was accentuated by Sirt1 inhibition (Luo *et al.*, 2001; Vaziri *et al.*, 2001; Langley *et al.*, 2002; Cheng *et al.*, 2003).

*Senescence-like growth arrest was accompanied by attenuated activation of MAPK pathways in response to growth factors*

We examined the activation status of signaling pathways of MAPKs and Akt/PKB in response to growth factors, epidermal growth factor (EGF) and insulin-like growth factor-I (IGF-I). When untreated with Sirtinol, upon exposure to EGF or IGF-I, robust phosphorylation of extracellular-regulated protein kinase (ERK), c-Jun N-terminal kinase (JNK/SAPK, also termed stress-activated protein kinase) and p38 MAPK was observed in MCF-7 and H1299 cells. By contrast, in Sirtinol-treated senescent MCF-7 and H1299 cells at 10 days after the addition of Sirtinol (100 $\mu$M), basal (unstimulated) phosphorylation of ERK, JNK/SAPK and p38 MAPK was reduced compared with untreated cells (Figure 8). In addition, EGF- or IGF-I-stimulated phosphorylation of ERK, JNK/SAPK and p38 MAPK was attenuated in MCF-7 and H1299 cells at 10 days after the addition of Sirtinol, compared to untreated cells.

Reduced activation of ERK, JNK/SAPK and p38 MAPK was corroborated by the phosphorylation status of the endogenous substrates of these MAPKs. Basal (unstimulated) as well as EGF- or IGF-I-stimulated phosphorylation of Elk-1, c-Jun and ATF-2 was also decreased in Sirtinol-treated senescent MCF-7 and H1299 cells at 10 days after the addition of Sirtinol, compared with untreated cells (Figure 9). The protein expression of ERK, JNK/SAPK, p38 MAPK, Elk-1, c-Jun and ATF-2 did not differ between Sirtinol-treated and untreated MCF-7 and H1299 cells.

However, at 3 days after the addition of Sirtinol, unlike at 10 days after the inhibitor addition, EGF-stimulated phosphorylation of ERK, JNK/SAPK and p38 MAPK was not attenuated in MCF-7 cells, compared with untreated cells (Figure 8d). These results suggest that attenuated MAPK pathways may be a consequence, rather than a cause, of Sirtinol-induced commitment of senescence-like growth arrest.

In contrast, tyrosine phosphorylation of the receptors for EGF and IGF-I by their ligands was not altered by Sirtinol treatment in MCF-7 and H1299 cells at 10 days after the addition of Sirtinol (Figure 10). The expression of EGF receptor and IGF-I receptor did not differ between Sirtinol-treated and untreated cells. These findings suggest that the defects responsible for impaired activation of MAPKs may exist at the level(s) of postreceptor signaling cascades.

Ras plays a critical role in growth factor-stimulated activation of MAPK pathways. Active Ras was markedly increased by EGF in untreated MCF-7 and H1299 cells. In Sirtinol-treated senescent MCF-7 and H1299 cells, however, the basal (unstimulated) level of active Ras was reduced compared with untreated cells, and EGF failed to increase active Ras (Figure 11a). Consistent with defective activation of Ras, basal (unstimulated) and EGF- or IGF-I-stimulated phosphorylation of Raf-1, MEK, SEK1/MKK4 and MKK7 was attenuated in Sirtinol-treated cells relative to untreated cells (Figure 11b). However, no difference was found between Sirtinol-treated and untreated MCF-7 and H1299 cells in the protein expression of Ras, Raf-1, MEK, SEK1/MKK4 and MKK7.

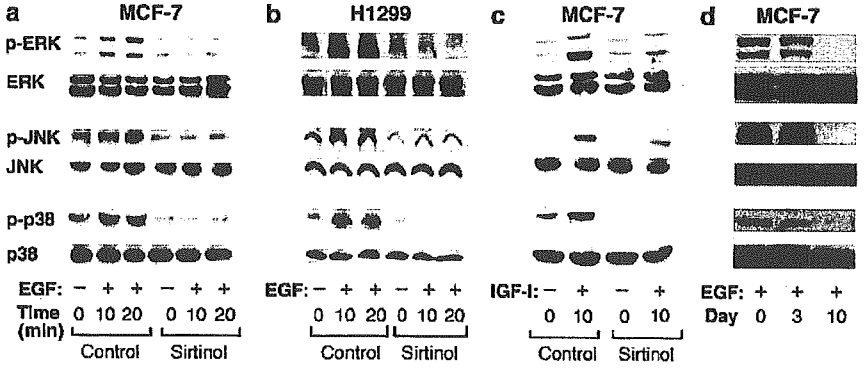


**Figure 8** Growth factor-stimulated phosphorylation of MAPKs in Sirtinol-treated cells. (**a–c**) At 10 days after the addition of Sirtinol (100 $\mu$M), following overnight serum starvation, the cells were exposed to EGF (50 ng/ml) for 10 or 20 min (**a**, **b**), or to IGF-I (100 ng/ml) for 10 min (**c**). In untreated (Control) MCF-7 and H1299 cells, marked phosphorylation of ERK, JNK/SAPK and p38 MAPK was induced by EGF or IGF-I. In Sirtinol-treated MCF-7 and H1299 cells, basal (unstimulated) as well as EGF- and IGF-I-stimulated phosphorylation of ERK, JNK/SAPK and p38 MAPK was decreased compared with untreated cells. (**d**) At 0, 3 and 10 days after the addition of Sirtinol (100 $\mu$M), MCF-7 cells were stimulated with EGF (50 ng/ml) for 20 min. EGF-stimulated phosphorylation of ERK, JNK/SAPK and p38 MAPK was markedly impaired at 10 days, but preserved at 3 days after the addition of Sirtinol.